L. Glaser

L. 格拉泽

Contents

目录

Abstract

摘要

This review introduces Markov Chain Monte Carlo simulations in causal set theory, with a focus on the study of the 2d orders. It will first introduce the Benincasa-Dowker action on causal sets and cover some musings on the philosophy of computer simulations. It then proceeds to review results from the study of the 2d orders, first their general phase transition and scaling behavior and then results on defining a wave function of the universe using these orders and on coupling the 2 d orders to an Ising like model. Including matter of this type shows a strong coupling between matter and geometry, which leads to new phase transitions. However, while the matter does induce a new phase transition, it does not change the order of the phase transition of geometry.

本综述介绍因果集合论中的马尔可夫链蒙特卡洛模拟，聚焦二维序的研究。本文将首先介绍因果集合上的贝宁卡萨-道克作用量，并探讨计算机模拟的相关哲学思考。随后回顾二维序的研究成果: 先介绍其一般相变与标度行为，再介绍利用这些序定义宇宙波函数，以及将 2 d 序耦合到类伊辛模型的相关结果。纳入该类型物质表明物质与几何之间存在强耦合，这会催生新的相变。然而尽管物质确实会诱发新的相变，但不会改变几何本身相变的阶。

L. Glaser (☑)

L. 格拉泽 (☑)

University of Vienna, Vienna, Austria

奥地利维也纳维也纳大学

e-mail: l.glaser@univie.ac.at

邮箱:l.glaser@univie.ac.at

Keywords

关键词

Quantum gravity · Path integral · Causal sets · Computer simulations · 2d orders

量子引力 · 路径积分 · 因果集合 · 计算机模拟 · 二维序

Introduction

引言

A causal set is space-times reduced to a discrete causal structure. To develop a theory of quantum gravity based on such a discretization requires us to quantize the dynamics of the theory. The natural language for this is a path integral that sums over causal sets. To non-perturbatively study this path sum we can use computer simulations.

因果集是约化为离散因果结构的时空。要建立基于这种离散化的量子引力理论，我们需要对该理论的动力学进行量子化。实现这一点的自然方式是对所有因果集求和的路径积分。为了对该路径求和进行非微扰研究，我们可以借助计算机模拟。

To study the path integral, which is fundamentally a quantum theory of Lorentzian space-times, using computer simulations, it is turned into a statistical sum over Lorentzian space-times. This is necessary since the causal set equivalent of the Einstein-Hilbert action is purely real and would thus lead to a complex weight factor, which is difficult to sample numerically.

路径积分本质上是洛伦兹时空的量子理论，为了用计算机模拟研究它，我们将其转换为对洛伦兹时空的统计求和。这一转换是必要的，因为爱因斯坦-希尔伯特作用量的因果集等价形式是纯实的，会产生难以进行数值采样的复权重因子。

Aside from the numerical methods focussed at in this review, there are other paths to understand how causal sets can make up our universe. For a full picture of the quantum theory we would like a covariant dynamics motivated intrinsically through the causal set, this approach is described more in the P Chap. 71, ”Covariant Growth Dynamics” written by Stav Zalel. Another approach toward defining the quantum dynamics are sequential growth models, which constructs causal sets element by element, and thus defines a measure on the space of all causal set, as introduced by Rideout and Sorkin in [1].

除了本综述重点介绍的数值方法外，还有其他研究方向可以探索因果集如何构成我们的宇宙。要得到量子理论的完整图景，我们需要由因果集内在驱动的协变动力学，Stav Zalel 撰写的第 71 章“协变增长动力学”对该方向做了更详细的介绍。另一种定义量子动力学的方法是顺序增长模型，该模型逐元素构建因果集，从而在所有因果集的空间上定义测度，这一方法由 Rideout 和 Sorkin 在文献 [1] 中提出。

This chapter will focus on computer simulations of a model system of causal sets, the 2d orders. In the section ”Entropy vs Energy, the Struggle of the Path Integral,” we will discuss the interplay of entropy and action on the space of all partial orders, which is dominated by the Kleitman Rothschild orders, described in section ”Kleitman Rothschild Orders” and then introduce the 2d orders as a restricted class of partial orders which are of special interest in causal set theory, in section ”2d Orders as Causal Sets.” This section closes with a short review of how the action on causal sets is derived, section ”Energy - An Action for a Causal Set,” and in section ”Markov Chain Monte Carlo Simulations” introduce Markov Chain Monte Carlo Simulations,

the main technical tool used in simulating causal set theory. Section ”Simulations of 2d Orders” introduces computer simulations on the 2d orders and splits into three subsections, each focussing on a different aspect. The first section ”A First Order Phase Transition” describes the simulations of pure 2d orders, the study of their phase transitions and scalings. The next section ”The Wave Function of a Universe” describes work on computer simulations of a Hawking-Hartle wave function in the 2d orders, and the last section ”Adding Matter - The Ising Model” describes results on the 2d orders coupled to the Ising model. This chapter closes with a short outlook section ”Outlook” on other open questions in simulations of the 2 d orders and possible extensions of the model.

本章重点研究因果集模型系统——二维序的计算机模拟。在“熵与能量: 路径积分的困境”一节中，我们将讨论所有偏序空间上熵与作用量的相互影响，该空间由 Kleitman-Rothschild 序主导，我们会在“Kleitman-Rothschild 序”一节对此进行描述，随后在“作为因果集的二维序”一节介绍二维序，它是偏序集中一个受限制的类别，在因果集理论中具有特殊研究价值。本章在“能量: 因果集的作用量”一节简要回顾了因果集上作用量的推导过程，在“马尔可夫链蒙特卡洛模拟”一节介绍了模拟因果集理论的核心技术工具——马尔可夫链蒙特卡洛模拟。“二维序的模拟”一节介绍了针对二维序的计算机模拟，该节分为三个子部分，每个子部分聚焦一个不同的研究方向。第一个子部分“一级相变”介绍了纯二维序的模拟，以及对其相变和标度性质的研究。下一个子部分“宇宙的波函数”介绍了在二维序中对霍金-哈特利波函数的计算机模拟研究，最后一个子部分“加入物质: 伊辛模型”介绍了二维序耦合伊辛模型的研究结果。本章最后在“展望”一节简要展望了 2 d 序模拟中的其他开放性问题以及模型的可能扩展方向。

Entropy vs Energy, the Struggle of the Path Integral

熵对能量，路径积分的困境

Exploring the path integral over a theory of quantum gravity in computer simulations means studying the interplay between the entropy in the space of configurations and the action assigned to these configurations. Changing the class of configurations can lead to a momentous change in the path integral, as impressively demonstrated by causal dynamical triangulations (CDT) [2]. While the input of CDT and dynamical triangulations (DT) is almost identical, the restriction of the path integral in CDT to only those configurations which allow for a definite time direction at each point, by imposing a preferred time foliation, changes the path integral completely. While DT does not show a phase transition of higher order and thus does not allow for a continuum limit, CDT does not only have such a phase transition but also has a phase adjacent to this transition that shows 4 d continuum like behavior.

在计算机模拟中探索量子引力理论的路径积分，本质是研究组态空间中的熵与这些组态对应的作用量之间的相互影响。改变组态的类别会给路径积分带来重大改变，因果动态三角剖分 (CDT)[2] 就有力地证明了这一点。CDT 和动态三角剖分 (DT) 的输入几乎完全一致，但 CDT 通过施加优先时间叶状结构，将路径积分限制在仅满足每个点都存在确定时间方向的组态中，这就彻底改变了路径积分的结果。DT 不存在高阶相变，因此无法取连续极限；而 CDT 不仅存在这类相变，在该相变相邻的相中还表现出 4 d 类连续统行为。

It is thus clear that explorations of the path integral over causal sets will need to consider both which class of causal sets to weight them with. This entropy of configurations is baked into the configuration space,

it is the entropy on the space of all causal sets, so the counting of partial orders.

因此很明显，探索因果集路径积分时，必须同时考虑对哪一类因果集进行加权。组态熵内生于组态空间，它是整个因果集空间的熵，对应于偏序的计数。

Kleitman Rothschild Orders

克莱特曼-罗斯柴尔德序

Mathematically speaking, a causal set is a partial order, and in the mathematical literature on partial orders, there is an impressive result by Kleitman and Rothschild, concerning the number of possible partial orders. In [3] they show that, in the large N limit, the number of possible partial orders goes like $N^2/4$. They prove this by establishing that this is the number of a particular type of three-layer order, which dominates the number of all partial orders. These orders, often called Kleitman Rothschild (KR) orders, are defined as follows: they consist of three layers, L_1, L_2, L_3 , with $N/4 + \mathcal{O}\left(N^{1/2}\log N\right)$ elements in layers L_1, L_3 and $N/2 + \mathcal{O}\left(N^{1/2}\log N\right)$ elements in layer L_2 . Each element in layer L_2 is to the future of half of the elements of L_1 and the past of half of the elements of L_3 , and thus all elements of L_1 are in the past of all elements of L_3 . An example of a 20 element KR order is shown in Fig. 1.

从数学角度来说，因果集是一个偏序集，在偏序集的数学研究中，克莱特曼和罗斯柴尔德得到了一个关于偏序集总数的重要结论。在文献 [3] 中，他们证明了，在大 N 极限下，偏序集的总数满足 $N^2/4$ 。他们通过证明该计数对应一种特殊三层偏序集得到结论，这类偏序集在所有偏序集中占主导地位。这类偏序集通常被称为克莱特曼-罗斯柴尔德序 (KR 序)，其定义如下: 它由三层构成，即 L_1, L_2, L_3 ，L_1, L_3 层有 $N/4 + \mathcal{O}\left(N^{1/2}\log N\right)$ 个元素，L_2 层有 $N/2 + \mathcal{O}\left(N^{1/2}\log N\right)$ 个元素。L_2 层的每个元素都位于 L_1 一半元素的未来、L_3 一半元素的过去，因此 L_1 的所有元素都在 L_3 所有元素的过去。图 1 展示了一个 20 元素克莱特曼-罗斯柴尔德序的例子。

This mathematical result concerns the large N limit, which leaves the question of how large N can be before the KR orders dominate. To explore this, Henson et al. [4] used Monte Carlo simulations to sample the space of all causal sets. They found that KR orders are already $> 90\%$ of the orders sampled for $N = 85$, which indicates that the large N regime is already reached. Since our universe consists of, assuming each element to be of Planck volume, roughly 10^{240} elements, the most likely partial orders of the size of the universe are clearly KR orders.

该数学结论仅针对大 N 极限，仍存在一个问题: 多大的 N 才能让 KR 序占据主导。为探究这个问题，亨森等人 [4] 采用蒙特卡洛模拟对所有因果集的空间采样。他们发现，当 $N = 85$ 时，采样得到的偏序集中已经有 $> 90\%$ 是 KR 序，这说明大 N 区域已经达到。如果假设每个元素的体积为普朗克体积，我们的宇宙大约包含 10^{240} 个元素，因此这个宇宙尺寸下最可能的偏序集显然就是 KR 序。

Fig. 1 Example of a 20 element Kleitman Rothschild order

图 1 一个 20 元素克莱特曼-罗斯柴尔德序的示例

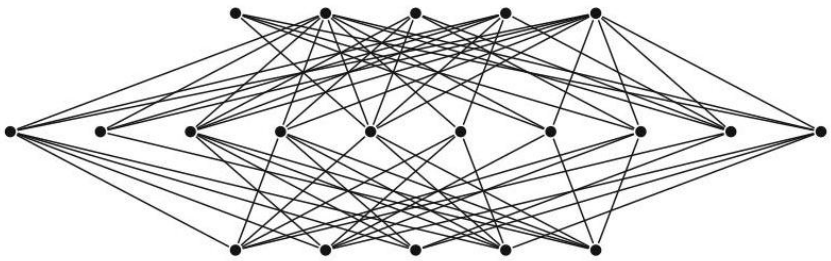

The entropy on the space of all causal sets is thus not in favor of manifoldlike causal sets, requiring a large energy to suppress these in the statistical path integral, as studied in computer simulations. There is, however, hope that the case is different for the complex path integral. It is possible to show that the integral over KR orders is suppressed by actions for which the number of links is the leading term [5], as is the case for most casual set actions, as introduced below.

因此，所有因果集空间的熵并不偏向类流形因果集，要在统计路径积分中压制 KR 序需要很大的能量，计算机模拟中已经对该情况进行了研究。但复路径积分的情况仍有转机。可以证明，对于大多数下文将介绍的因果集作用量而言，连接数是作用量的主导项，对 KR 序的积分会被这类作用量压制 [5]。

2d Orders as Causal Sets

作为因果集的二维序

The class of all partial orders is very large, and as we discussed above dominated by the KR orders. This motivated the search for a useful subclass of partial orders to study using numerics. This class was found in [6] to be the 2 d orders, defined in [7]. A N element 2 d order starts with the set S or integers from 1 to N , and two sets of labels $U = (u_1, u_2, ... u_N), V = (v_1, v_2, ... v_N)$ with $u_i, v_i \in S$ and $u_i \neq u_j, v_i \neq v_j$ unless $i = j$. The sets U, V are then total orders, with their ordering induced from the ordering on S , and we define a N element $2d$ order as the intersection $C = U \cap V$. So $e_i \prec e_j$ iff $u_i < u_j$ and $v_i < v_j$, a useful example of such a $2d$ order is a set of events in $2d$ Minkowski space-times, for which no u_i or v_i coincide.

所有偏序构成的集合规模极大，且正如我们前文讨论过的，KR 序在其中占主导地位。这推动了人们寻找一个可用数值方法研究的偏序有用子类。文献 [6] 指出这个子类就是定义于文献 [7] 的 2 d 序。一个 N 元 2 d 序起始于集合 S ，即 1 到 N 的整数，以及两套标签 $U = (u_1, u_2, ... u_N), V = (v_1, v_2, ... v_N)$ ，满足 $u_i, v_i \in S$ ，且除非 $i = j$ 否则都满足 $u_i \neq u_j, v_i \neq v_j$ 。集合 U, V 本身是全序，它们的序由 S 上的序诱导而来，我们将 N 元 $2d$ 序定义为交集 $C = U \cap V$ 。因此 $e_i \prec e_j$ 当且仅当 $u_i < u_j$ 且 $v_i < v_j$ 。这类 $2d$ 序一个典型的有用例子就是二维闵氏时空中的事件集合，其中没有 u_i 或 v_i 重合。

The 2d orders have several advantages for numerical studies of partial orders. One is that, while they include a large variety of non-manifoldlike partial orders, it can be shown that the ”most likely” 2d orders all faithfully embed into 2d Minkowski space [6,7]. These faithfully embedding orders are often also referred to as random orders. They are thus a model that allows us to study space-times of a fixed dimension through causal set theory. In addition, the labelling by two numbers defines an embedding into 2d Minkowski space and thus allows us to plot the orders we study and provides an additional tool to understand the system.

二维序在偏序的数值研究中有诸多优势。其一，尽管二维序包含大量非流形类偏序，可证明“最概然”的二维序都能忠实嵌入二维闵氏空间 [6,7]。这些可忠实嵌入的序通常也被称为随机序。因此它们是一个可供我们通过因果集理论研究固定维度时空的模型。此外，两个数的标记本身就定义了一个到二维闵氏空间的嵌入，因此我们可以绘制所研究的序，为理解该系统提供额外工具。

Energy - An Action for a Causal Set

能量——因果集的作用量

Since we have covered the entropy part of the story, it is now time to think about the energy of a causal set. To take a path sum over causal sets, we need to define a causal set action that weights the individual causal sets. In principle, we have complete freedom to define the action; however, to recover general relativity in the limit of manifoldlike causal sets, it seems prudent to demand that the action should approximate the Einstein-Hilbert action in this case.

既然我们已经介绍了这一理论中的熵部分，现在是时候讨论因果集的能量了。要对因果集进行路径求和，我们需要定义一个给单个因果集赋予权重的因果集作用量。原则上，我们完全可以自由定义作用量；但为了在类流形因果集的极限下得到广义相对论，要求作用量在此情形下近似爱因斯坦-希尔伯特作用量是合理的。

While it should be possible to reconstruct the scalar curvature, and thus the Einstein-Hilbert action, from many different measures on the causal set, one of the easiest ways to do so is to start from the d'Alembertian operator. To define a discretized derivative on the causal set, we need to rely purely on relativistically covariant information. In this case we write a retarded d'Alembertian operator, at an element x by using the past of the element. In 2 dimensions the expression is

尽管我们可以从因果集的许多不同测度重构标量曲率，进而得到爱因斯坦-希尔伯特作用量，但最简单的方法之一是从达朗贝尔算子出发。要在因果集上定义离散导数，我们只能依赖相对论协变信息。为此，我们利用元素的过去，在元素 x 处写出推迟达朗贝尔算子。在二维下表达式为

$$B^{(2)}\phi(x) := \frac{1}{l^2}\left[-2\phi(x) + 4\left(\sum_{y\in L_0(x)}\phi(y) - 2\sum_{y\in L_1(x)}\phi(y) + \sum_{y\in L_2(x)}\phi(y)\right)\right], \tag{1}$$

where $L_i(y)$ are all elements y of the causal set for which $|I_A(x,y)| = i$, with $I_A(x,y)$ the Alexandrov interval, consisting of all elements causally between x, y [8, 9] . The pre-factor $\frac{1}{l^2}$ is for dimensional reasons, with l^d the d -dimensional discreteness volume. This is a sum over "layers" of the causal set, where using the Alexandrov intervals to define the layers makes these covariant. The 2 d expression above can be generalized to arbitrary dimension [10, 11] ,

其中 $L_i(y)$ 是满足 $|I_A(x,y)| = i$ 的因果集中所有元素 y ，$I_A(x,y)$ 是亚历山德罗夫区间，由所有因果上位于 x, y [8, 9] 之间的元素构成。前置因子 $\frac{1}{l^2}$ 出于量纲考虑，l^d 是 d 维离散体积。这是对因果集“层”的求和，用亚历山德罗夫区间定义层可以保证这些层是协变的。上述 2 d 表达式可以推广到任意维数 [10, 11] ,

$$B^{(d)}\phi(x) = \frac{1}{l^2}\left(\alpha_d \phi(x) + \beta_d \sum_{i=0}^{n_d} C_i^{(d)} \sum_{y \in L_i} \phi(y)\right), \tag{2}$$

where $\alpha_d, \beta_d, C_i^{(d)}$, and n_d are dimension dependent constants.

其中 $\alpha_d, \beta_d, C_i^{(d)}$ ， 且 n_d 是依赖于维数的常数。

To determine these constants, we demand that this expression agrees with the d'Alembertian operator, when applied to a casual set sprinkled into flat Minkowski space.

为确定这些常数，我们要求当该表达式作用于撒入平直闵氏空间的因果集时，与连续的达朗贝尔算子一致。

For such a causal set, the number of points in the i -th layer is

对于这类因果集，第 i 层内的点数量为

$$L_i(y) = \int_{J^-(0)} \mathrm{d}V_y \frac{\left(l^{-d} V_d(y)\right)^i}{i!} e^{-l^{-d} V_d(y)} \tag{3}$$

which we can insert above, to write down a continuum operator

我们可以将其代入上式，写出连续算子

$$l^2\left(\Box_l^{(D)}\phi\right)(x) = \alpha_d \phi(x) + \sum_{i=0}^{L_{\max}} \frac{\beta_d C_i^{(d)}}{i!} \int_{J^-(x)} e^{-l^{-d} V(x,y)} \left(l^{-d} V(x,y)\right)^i \phi(y)\, \mathrm{d}V_y.$$

(4)

The constants $C_i^{(d)}$ can be generated through differential operators $\mathcal{O}_d$ in the discreteness scale l , which for even dimension are defined as $\mathcal{O}_{2n} = \frac{1}{2^{n+1}(n+1)!}(2 - l\frac{\partial}{\partial l})\left(4 - l\frac{\partial}{\partial l}\right)\ldots\left(2n+2 - l\frac{\partial}{\partial l}\right)$ and $\mathcal{O}_{2n+1} = \mathcal{O}_{2n}$. Using this continuum approximation we can calculate

常数 $C_i^{(d)}$ 可通过离散标度 l 下的微分算子 $\mathcal{O}_d$ 得到，对于偶维，它们定义为 $\mathcal{O}_{2n} = \frac{1}{2^{n+1}(n+1)!}(2 - l\frac{\partial}{\partial l})\left(4 - l\frac{\partial}{\partial l}\right)\ldots\left(2n+2 - l\frac{\partial}{\partial l}\right)$ 和 $\mathcal{O}_{2n+1} = \mathcal{O}_{2n}$ 。利用该连续近似我们可以计算

$$\frac{1}{\beta_d} = \lim_{l\to 0} \frac{1}{2l^{d+2}} \mathcal{O}_d \int \mathrm{d}V_y \left(\frac{v_y - u_y}{\sqrt{2}}\right)^2 e^{-l^{-d} V_{0d}(y)} \tag{5}$$

$$\frac{\alpha_d}{\beta_d} = -\lim_{l\to 0} \frac{1}{l^d} \mathcal{O}_d \int \mathrm{d}V_y e^{-l^{-d} V_{0d}(u,v)}. \tag{6}$$

This can be solved to find

求解后可得

$$\alpha_d = \begin{cases} \frac{-2c_d^{\frac{2}{d}}}{\Gamma\left(\frac{d+2}{d}\right)} & \text{for even } d \\ \frac{-c_d^{\frac{2}{d}}}{\Gamma\left(\frac{d+2}{d}\right)} & \text{for odd } d \end{cases} \quad \beta_d = \begin{cases} \frac{2\Gamma\left(\frac{2}{d}+2\right)\Gamma\left(\frac{1}{d}+1\right)}{\Gamma\left(\frac{2}{d}\right)\Gamma(d)} c_d^{\frac{2}{d}} & \text{for even } d \\ \frac{d+1}{2^{d-1}\Gamma\left(\frac{2+d}{d}\right)} c_d^{\frac{2}{d}} & \text{for odd } d \end{cases}, \tag{7}$$

where $c_d = S_{d-2}\frac{2^{\frac{2-d}{2}}}{d(d-1)}$ with S_{d-2} the volume of the unit $d-2$ sphere.

其中 $c_d = S_{d-2}\frac{2^{\frac{2-d}{2}}}{d(d-1)}$，$S_{d-2}$ 是单位 $d-2$ 球面的体积。

As Sorkin already realized in [8], this expression has the correct expectation value. However, in the high-density limit, the fluctuations around this mean increase. He then proposed to resolve this issue by introducing an intermediate non-locality scale, and defining, for each d , a one parameter family of operators on scalar fields on a causal set

正如索金在文献 [8] 中已经认识到的，该表达式具有正确的期望值。然而，在高密度极限下，平均值周围的涨落会增大。随后他提出了解决该问题的方案: 引入一个中间非定域性标度，并对每个 d 定义因果集上标量场的单参数算符族

$$B_\varepsilon^{(d)}\phi(x) := \frac{\varepsilon^{\frac{2}{d}}}{l^2}\left(\alpha_d\phi(x) + \beta_d\varepsilon\sum_{y\prec x} f_d\left(I_A(x,y),\varepsilon\right)\phi(y)\right), \tag{8}$$

where the sum is over all elements y in the causal set to the past of x and

其中求和遍历因果集中位于 x 过去的所有元素 y，且

$$f_d(n,\varepsilon) := (1-\varepsilon)^n \sum_{i=1}^{n_d} C_i^{(d)} \binom{n}{i-1} \left(\frac{\varepsilon}{1-\varepsilon}\right)^{i-1}, \tag{9}$$

where $\varepsilon = V_{Pl}/V, V_{Pl} = l^d$ is the Planck volume, and V is the volume of the intermediate non-locality scale. In the limit of $V \to V_{Pl}$, this agrees with equation (2) above, which corresponds to the action with minimal non-locality. For larger V/ smaller ε , the smearing function $f_d(n,\varepsilon)$ becomes less local and includes more layers, as illustrated in Fig. 2. This suppresses the fluctuations of the operator.

其中 $\varepsilon = V_{Pl}/V, V_{Pl} = l^d$ 是普朗克体积，V 是中间非定域性标度的体积。在 $V \to V_{Pl}$ 的极限下，这与上文的式 (2) 一致，对应最小非定域性的作用量。对于更大的 V/ smaller ε，抹平函数 $f_d(n,\varepsilon)$ 的定域性变弱，包含更多层，如图 2 所示。这会抑制该算符的涨落。

To derive an expression for the scalar curvature from this, we generalize from calculating the d'Alembertian on Minkowski space to a curved space-times. We can use a Riemann normal coordinate expansion to derive that

为了由此推导出标曲率的表达式，我们将计算闵氏空间达朗贝尔算符的方法推广到弯曲时空。我们可以利用黎曼法坐标展开推导出

$$\lim_{l\to 0}\bar{B}^{(d)}\phi(x)=\Box^{(d)}\phi(x)+\frac{1}{2}R(x)\phi(x). \tag{10}$$

When applying this operator to a constant scalar field $\phi(x)=2$, the only contributing term is the scalar curvature at a given point. To derive the Einstein-Hilbert action, we integrate this over space-times, which in the case of the causal set is a sum over all causal set elements. Assuming the discreteness is at the Planck scale $l=l_p$, this leads to the following expression [10],

将该算符作用于常数标量场 $\phi(x)=2$ 时，唯一有贡献的项是给定点的标曲率。为了推导出爱因斯坦-希尔伯特作用量，我们对时空做积分，对于因果集而言，积分即为对所有因果集元素求和。假设离散性存在于普朗克标度 $l=l_p$，由此得到如下表达式 [10],

$$\frac{1}{\hbar}S_{dD}=\alpha_d N+\beta_d\sum_{i=1}^{n_d}C_i^{(d)}N_i \tag{11}$$

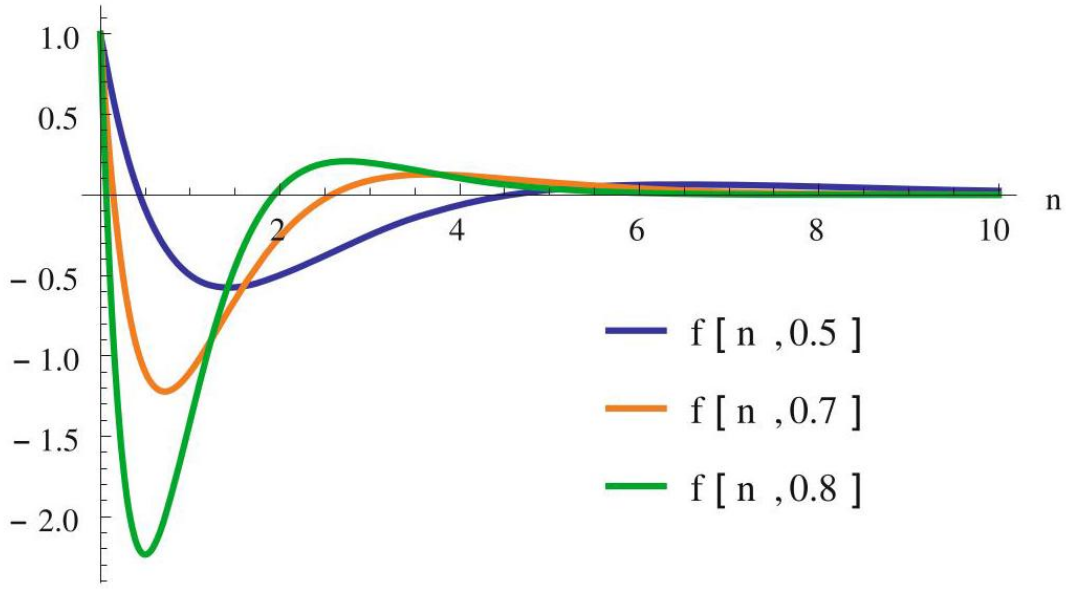

Fig. 2 Plot of the smoothing function $f(n,\varepsilon)$ for 2 d and different values of ε

图 2 $f(n,\varepsilon)$ 在 2 d 和不同 ε 取值下的平滑函数图像

for a N element causal set, where the numbers N_i are the abundances of i intervals, which can be calculated analytically [12]. In addition to their use in the action, these abundances are also useful as measures of manifold likeness of a causal set and as measures of locality for subregions of a causal set.

对应含 N 个元素的因果集，其中数 N_i 是 i 区间的丰度，该丰度可解析计算 [12]。除了用于作用量，这些丰度还可用于衡量因果集的流形相似性，以及衡量因果带子区域的定域性。

In the case of $d=2$, which is used in the simulations we will talk about, this leads to

对于我们后文将要讨论的模拟中所使用的 $d=2$，可得

$$\frac{1}{\hbar}S_{2D} = N - 2N_0 + 4N_1 - 2N_2 \tag{12}$$

for $\varepsilon = 1$ and

对应 $\varepsilon = 1$，且

$$\frac{1}{\hbar}S_{2D}(\varepsilon) = 4\varepsilon\left(N - 2\varepsilon\sum_{n=0}^{N-2} N_n f_2(n,\varepsilon)\right) \tag{13}$$

$$f_2(n,\varepsilon) = (1-\varepsilon)^n\left(1 - \frac{2\varepsilon n}{(1-\varepsilon)} + \frac{\varepsilon^2 n(n-1)}{2(1-\varepsilon)^2}\right) \tag{14}$$

for arbitrary ε. In the computer simulations, the non-locality parameter ε is a free input and thus defines a class of actions.

对任意 ε 成立。在计算机模拟中，非定域性参数 ε 是自由输入参数，因此定义了一类作用量。

Markov Chain Monte Carlo Simulations

马尔可夫链蒙特卡洛模拟

In a quantum theory, states do not have a statistical weight, instead they have a quantum amplitude. The usual solution when applying simulations like this to quantum gravity systems is to introduce a Wick rotation, going from a quantum Lorentzian system to a statistical Euclidean system. Since causal set theory is intrinsically Lorentzian, this is not possible, instead we introduce an inverse temperature parameter β which we analytically continue $\beta \to i\overline{\beta}$

在量子理论中，态不具有统计权重，而是具有量子振幅。将这类模拟应用于量子引力系统时，常用解决方案是引入威克转动，将量子洛伦兹系统转换为统计欧几里得系统。由于因果集理论本质上是洛伦兹型的，该方法无法适用，因此我们引入一个逆温度参数 β 并对其进行解析延拓 $\beta \to i\overline{\beta}$

$$e^{i\beta S_{CST}} \to e^{-\overline{\beta}S_{CST}}. \tag{15}$$

The parameter β now becomes a new free parameter of our theory. Some of the philosophy about why a parameter Wick rotation is useful in this context has been developed in [13].

参数 β 由此成为我们理论的一个新自由参数。文献 [13] 已经阐述了为何参数威克转动在该场景下有用的部分基本思路。

The studies described in this chapter are all done using Markov Chain Monte Carlo (MCMC) simulations, which are a tool for importance sampling from a large class of objects. They are often used in statistical physics applications, since they allow us to probe large sample spaces efficiently by favoring the regions that contribute most to the state sum. They do so by sampling the state space through a Markov Chain, generated using an ergodic set of moves through state space.

本章所述研究全部通过马尔可夫链蒙特卡洛 (MCMC) 模拟完成，该模拟是从一大类对象中进行重要性采样的工具。它常被用于统计物理研究，因为通过优先覆盖对态求和贡献最大的区域，它能让我们高效探测大样本空间。它借助遍历性的态空间移动生成马尔可夫链，通过该链对态空间采样实现上述功能。

An example of such a move, for our system of the 2d orders, is the coordinate flip move, first constructed in [14]. It uses the u_i, v_i labels of the orders, to propose a new order by flipping one of the coordinates.

对于我们的二维序系统，这类移动的一个例子是坐标翻转移动，最早由文献 [14] 构造。它利用序的 u_i, v_i 标记，通过翻转其中一个坐标来提议一个新序。

1. Randomly pick two of the N elements (u_1, v_1) and (u_2, v_2) of the causal set.

1. 随机选取因果集的 N 个元素 (u_1, v_1) 和 (u_2, v_2) 。

2. Randomly pick one of the two labels $a \in (u, v)$, corresponding to one of the two light-cone directions.

2. 随机选取两个标记 $a \in (u, v)$ 中的一个，对应两个光锥方向中的一个。

3. The proposed new causal set is the 2 d order with the labels a_1, a_2 interchanged.

3. 提议的新因果集是交换标记 a_1, a_2 后的 2 d 序。

This move is clearly ergodic in the space of 2 d orders and easy to implement on the computer. Code using this move to simulate the 2d orders, together with an added matter coupling, as described below can be found in [15].

该移动在 2 d 序空间中显然具有遍历性，且易于在计算机上实现。文献 [15] 中可以找到使用该移动模拟二维序、并加入下文所述物质耦合的代码。

The MCMC algorithm most often used in quantum gravity theories is Metropolis Hastings, as for example explained in [16]. The algorithm starts at some configuration of the system s_1 ; from this initial state, the algorithm generates a new state, using the prescribed moves (The exact initial configuration is in theory irrelevant, since it can be proven that for long enough running times the algorithm will converge toward the correct sampling probability for all states. In practice, the choice of initial configuration can massively slow down the convergence of the algorithm, and ensuring that the algorithm has converged toward the correct sampling is a non-trivial task. We will not go into more detail on this here but refer again to the excellent textbook by Newman and Barkema [16].). It is important that the set of moves is ergodic to ensure that the entire space of states can be sampled. After a new state is generated, the algorithm will append either the new state or an additional copy of the current state to the chain. The transition probability between the current state s_1 and a new proposed state s_2 in the chain is given by their statistical weight.

量子引力理论中最常用的 MCMC 算法是梅特罗波利斯-黑斯廷斯算法，例如文献 [16] 中有相关讲解。算法从系统 s_1 的某个构型出发；从该初始态开始，算法通过规定移动生成新态 (理论上初始构型无关紧要，因为可以证明，只要运行时间足够长，算法会收敛到所有态的正确采样概率；但实践中初始构型的选择会大幅拖慢算法收敛，且确保算法收敛到正确采样并非易事。我们在此不再展开，再次推荐读者阅读 Newman 与 Barkema 的优秀教材 [16])。移动集合具有遍历性对确保整个态空间都能被采样十分重要。生成新态后，算法会将新态或当前态的额外副本追加到链中。链中当前态 s_1 与提议新态 s_2 之间的转移概率由二者的统计权重给出。

If the new state has a higher statistical weight (lower energy) than the current state, it will always be accepted. Even if the new state has a lower statistical weight (higher energy), it has a chance of being accepted, with probability $\exp\left(S_{\text{old state}} - S_{\text{new state}}\right)$. This is important to avoid the chain getting stuck in a state that is a local minimum, in relation to the states that are adjacent to it under the set of moves, but which is not a global minimum.

如果新态的统计权重高于当前态 (能量更低)，它总会被接受。即使新态统计权重更低 (能量更高)，它也有概率被接受，概率为 $\exp\left(S_{\text{old state}} - S_{\text{new state}}\right)$。这对于避免链卡在局部极小值态十分重要: 这类态相对于移动集合可到达的邻态是极小值，但并非全局极小值。

Simulations of 2d Orders

二维序的模拟

This section will study three different explorations of the 2d orders using MCMC simulations. The first section ”A First Order Phase Transition” is about the phase diagram of the 2d orders, their remarkably simple scaling behavior, and their first-order phase transition. The second section ”The Wave Function of a Universe” is about an attempt to use the 2d orders to study a toy model of a wave function of the universe, transitioning from nothing to fixed size in the causal set, and the last section ”Adding Matter - The Ising Model” explores how the phase structure of the 2d orders changes when they are coupled to an Ising model.

本节将通过 MCMC 模拟研究三种不同的二维序探索工作。第一节“一级相变”围绕二维序的相图、其格外简单的标度行为以及它们的一级相变展开。第二节“宇宙波函数”介绍了利用二维序研究宇宙波函数玩具模型的尝试，该模型描述因果集中从无到固定尺寸的转变，最后一节“添加物质——伊辛模型”则探究了二维序耦合伊辛模型后其相结构的变化。

A First Order Phase Transition

一级相变

The first work on simulations of the 2d orders was done by Sumati Surya [14]. Careful study revealed that, using the action (12), the 2d orders show two distinct phases. Simulations for different values of ε and β make it possible to trace the phase transition line shown for $N = 50$ in Fig. 3.

二维序的模拟工作最早由 Sumati Surya 完成 [14]。细致研究表明，使用作用量 (12) 时，二维序呈现出两种截然不同的相。通过对 ε 和 β 取不同值进行模拟，我们可以描绘出图 3 中 $N = 50$ 对应的相变线。

The two phases are the random 2d orders and the crystalline orders, illustrated through insets in the figure. The low β phase is dominated by the random 2 d orders, which are the entropically favored states, while high β energetically favors the creation of layers. The energetically optimal state would be a set with two layers, thus maximizing the number of links; however, since this configuration exists exactly once, it is entropically strongly disfavored.

这两种相分别是随机二维序和晶体序，图中的插图已对其进行展示。低 β 相以随机 2 d 序为主，这类序是熵有利态；而高 β 在能量上有利于层结构的形成。能量最优态会是一个双层结构，因此可以最大化链接数量；但这种构型恰好只存在一种，因此在熵层面非常不利。

To delineate the different phases, a number of observables were used, the number of links, the value of the action, the height of the 2d order, the ordering fraction, time asymmetry, and the interval abundance [12]. The height is defined as the length of the longest chain, and the ordering fraction is the number of links, divided by the maximal number of links possible in a set of this size (which is $N(N-1)/2$, achieved exactly if the causal set consists of two equally sized layers where each element is connected to all elements in the other layer). The time asymmetry is measured by proxy, as the difference between the number of maximal and minimal elements in the causal set. The action of the system is time reversal invariant; it is thus interesting to see whether the dynamics of the system will break this invariance.

为了区分不同的相，研究使用了多个可观测量: 链接数、作用量值、二维序高度、有序分数、时间不对称性以及区间丰度 [12]。高度定义为最长链的长度；有序分数为链接数除以该尺寸集合中可能存在的最大链接数 (该最大值为 $N(N-1)/2$ ，当因果集恰好由两个大小相等的层构成，且每个层中的元素都与另一层所有元素相连时即可达到该最大值)。时间不对称性通过代理变量测量，即因果集中极大元与极小元数量之差。系统的作用量满足时间反演不变性，因此研究系统动力学是否会破坏这种不变性是很有意义的。

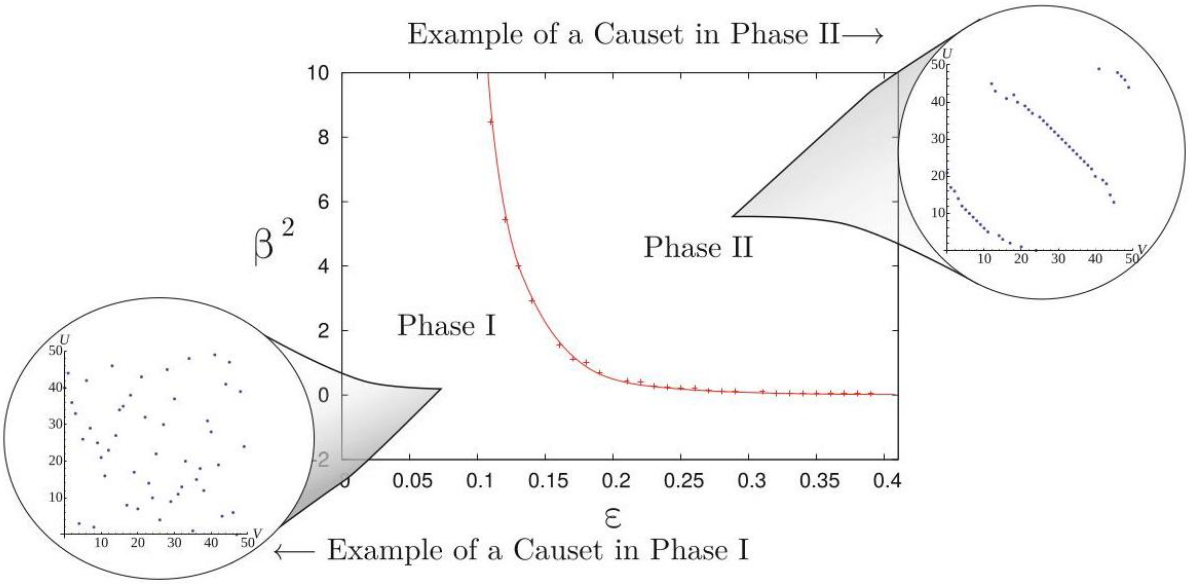

Fig. 3 Phase diagram for the 2 d orders in the ε, β^2 plane for $N = 50$. The insets show a typical causal set in either of the two phases to illustrate the dominant contribution. (Plot taken from [14] with slight modification to include images of the two phases)

图 3 $N = 50$ 对应的 2 d 序在 ε, β^2 平面中的相图。插图展示了两个相中典型因果集的样貌，以说明各自的主导特征。(图片改编自文献 [14]，添加了两个相的示意图)

The interval abundance is a particularly interesting observable that was first introduced in [14] and then studied in depth, analytically as well as numerically, in [12]. The interval abundance $I_A(n)$ counts the number of Alexandrov Intervals of size n . This defines a curve that can be calculated exactly for flat space and that contains a lot of information about the causal set. In particular, it can recognize the dimension of a region and recognize whether it is a locally flat region in a larger curved causal set. It can also be calculated for a slightly curved space-times [17].

区间丰度是一个非常值得关注的可观测量，它最早在文献 [14] 中提出，随后文献 [12] 从解析和数值层面进行了深入研究。区间丰度 $I_A(n)$ 统计大小为 n 的亚历山德罗夫区间的数量。由此得到的曲线可在平直空间中精确计算，且包含因果集的大量信息。该曲线尤其可以识别区域的维度，判断其是否为更大的弯曲因果集中的局部平直区域，也可对轻度弯曲时空计算该曲线 [17]。

Studying these quantities shows that the phase of random 2d orders has an ordering fraction of 0.5, an action of < 4, a height of 10, and no time asymmetry. All of these observations are in good agreement with those for a causal set generated through sprinkling into 2d Minkowski space and thus confirm that this is a continuum phase. This can also be tested using the interval abundance as a measure of manifoldlikeness [12].

对这些物理量的研究表明，随机二维序相的有序分数为 0.5，作用量小于 4，高度为 10，且不存在时间不对称性。所有这些观测结果都与泼入二维闵氏空间生成的因果集的结果高度吻合，因此证实该相是连续统相。这一点也可以通过用区间丰度度量流形相似性来检验 [12]。

The crystalline 2d orders on the other hand show clear non-manifoldlike behavior. They are energetically favored states with a large number of links and are marked by a relative high ordering fraction ~ 0.6 , a small action ~ -45 , a low height of just 3, and large time asymmetry, although the direction of the time asymmetry fluctuates.

另一方面，晶体二维序展现出明显的非流形行为。它们是能量有利态，拥有大量链接，特征为有序分数 ~ 0.6 相对较高、作用量 ~ -45 较小、高度仅为 3，且时间不对称性很大，尽管不对称性的方向存在涨落。

The existence of these two phases opens the question of what order the transition between them is. To study the order of a phase transition, one needs to perform a scaling analysis, comparing the behavior at the phase transition for different system sizes. This, together with a thorough analysis to understand how the system scales for varying in ε , was undertaken in [18].

这两个相的存在引出了一个问题: 它们之间的相变是几级相变？要研究相变的级数，需要进行标度分析，对比不同系统尺寸下相变处的行为。文献 [18] 完成了这项工作，同时也对 ε 变化时系统的标度行为进行了全面分析。

To explore the scaling, simulations were done for N between 30 and 90 and for ε from 0.1 to 0.5, covering an irregular grid of these values. The range for ε was chosen such since low and high ε are problematic. For very low values of ε , the system shows an additional phase, which was not studied in detail, since for very low ε at fixed size N the scale of the smearing of the action becomes much larger than the size of the set. For very high ε , the fluctuations in the action become strong, which requires much longer simulations to study.

为了探究标度行为，我们针对取值介于 30 到 90 之间的 N ，以及取值介于 0.1 到 0.5 之间的 ε 开展了模拟，覆盖了这些参数值的不规则网格。我们选择这一 ε 取值范围是因为低 ε 和高 ε 都存在问题: 当 ε 取值极低时，系统会出现一个额外的相，由于在固定 N 尺寸下，ε 极低时作用量弥散的尺度会远大于集合尺寸，因此本文没有对该相展开详细研究；当 ε 取值极高时，作用量的涨落会变得很强，这需要更长时长的模拟才能开展研究。

The first question explored was the type of the phase transition, which was determined to be of first order. This was done through exploration of the histogram of the action, and using the Binder coefficient [19]. The histograms are shown in Fig. 4a. The important observation here is that as N increases, the histogram at the phase transition splits further apart. At a higher order phase transition, the system at the phase transition point would show new, long range correlated, behavior and thus form a single peak as N increases. The Binder coefficient is defined as

我们探究的第一个问题是相变类型，最终确定该相变为一级相变。我们通过分析作用量直方图，并利用 Binder 系数 [19] 得到了这一结论。直方图如图 4a 所示。这里的核心观测结论是: 随着 N 增大，相变点处的直方图峰分裂得越来越开。如果是更高阶相变，相变点处的系统会呈现新的长程关联行为，因此随着 N 增大，直方图会形成单峰。Binder 系数定义如下

$$B = \frac{1}{3}\left(1 - \frac{\langle S^4 \rangle}{\langle S^2 \rangle^2}\right) \tag{16}$$

and is a useful tool to observe the order of a phase transition, exactly because of the behavior described above. For a higher order phase transition, this coefficient should go toward 0 as $N \to \infty$; the coefficient is shown in Fig. 4b.

且它正是由于上述特性，成为观测相变阶数的有效工具。对于更高阶相变，当 $N \to \infty$ 时，该系数会趋近于 0；该系数如图 4b 所示。

It is thus clear that the 2 d orders do not undergo a higher order phase transition. The existence of a higher order phase transition in a statistical system implies an infinite correlation length, and thus the existence of a continuum limit. Since causal sets are a fundamentally discrete theory, the lack of a higher order transition is not condemning in itself, as a continuum limit is explicitly not expected. It does, however, open interesting questions when observed from the vantage point of renormalization group techniques, where a higher order phase transition implies a universality of phenomena, which ensures that the fine structure at the Planck scale does not unduly influence physics at lower energies. Some first steps toward renormalization group techniques for causal sets are made in [20]. The lack of such a transition would then imply that there might

be no universality, which could lead to problems in the predictivity of causal sets. However, self averaging behavior, or other phenomena might resolve this difficulty, alternatively a more full description of causal sets might find a higher order transition after all. As shown in Fig. 5, the location of the phase transition β_c scales with $N\varepsilon^2$. In [18], this scaling was determined to be

因此可以明确，2 d 序不会发生更高阶相变。统计系统中存在高阶相变意味着关联长度趋于无穷，因此也意味着存在连续极限。由于因果集本身是基础离散理论，不存在高阶相变本身并不是致命问题——我们本来就不期望它存在连续极限。不过，从重整化群技术的视角来看，这确实引出了有意思的问题: 在重整化群框架下，高阶相变意味着现象满足普适性，这保证普朗克尺度的精细结构不会对低能物理产生过度影响。针对因果集的重整化群技术研究已经在文献 [20] 中完成了初步探索。如果不存在这类相变，那么就意味着可能不存在普适性，这会给因果集理论的可预测性带来问题。不过，自平均行为或其他现象或许能解决这一难题；换而言之，对因果集更完备的描述最终说不定还是能找到高阶相变。如图 5 所示，相变位置 β_c 随 $N\varepsilon^2$ 标度变化。文献 [18] 中确定的标度关系为

$$\beta_c\,(N,\varepsilon) = \frac{1.66^{(\pm 0.03)}}{N\varepsilon^2}$$

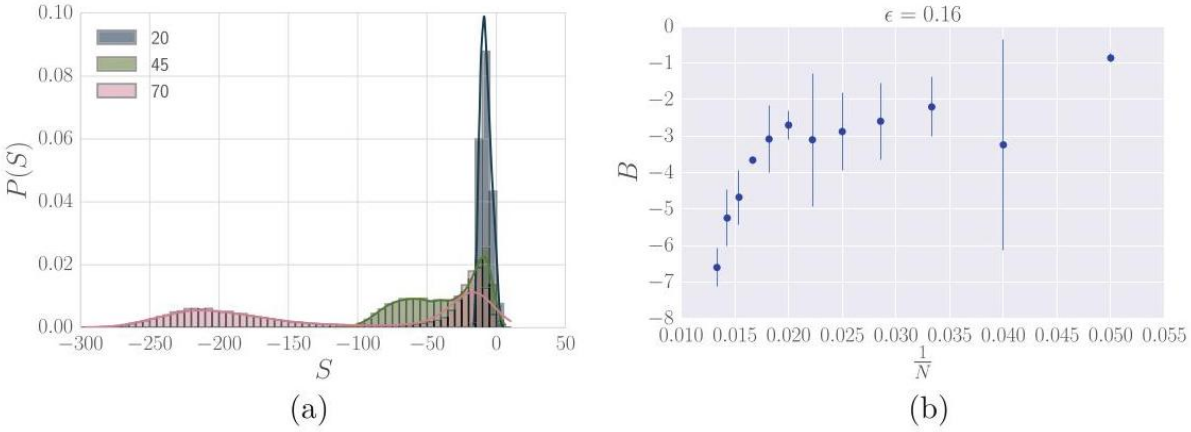

Fig. 4 The left-hand figure shows a histogram, depicting the occurrence of different action values in the simulations, showing that the system fluctuates between two different states, which become more different as the system size increases. This indication of a first-order phase transition is confirmed by the right-hand plot, which shows the Binder coefficient plotted against $1/N$. (a) Histogram demonstrating coexistence. (b) Binder coefficient

图 4 左图为直方图，展示了模拟中不同作用量值的出现频次，证明系统在两个不同状态之间涨落，且随着系统尺寸增大，两个状态的差异愈发明显。一级相变的这一指示得到了右图的确认，右图展示了 Binder 系数随 $1/N$ 的变化曲线。(a) 证明两相共存的直方图；(b) Binder 系数

plus some corrections in N^{-2} .

加上 N^{-2} 相关的一些修正项。

Not only does the location of the phase transition scale well, but the value of the action also shows very clear scaling behavior. To examine this behavior, we plot the action against the scale invariant temperature $\overline{\beta} = \beta N$. The action scales linearly with N for both the regions $\overline{\beta} < \overline{\beta}_c$ and $\overline{\beta} > \overline{\beta}_c$, as illustrated in Fig. 6.

不仅相变位置的标度行为表现良好，作用量的值也呈现出非常清晰的标度行为。为了检验这一行为，我们将作用量对标度不变温度 $\overline{\beta} = \beta N$ 作图。如图 6 所示，在 $\overline{\beta} < \overline{\beta}_c$ 和 $\overline{\beta} > \overline{\beta}_c$ 两个区域，作用量都与 N 呈线性标度关系。

For $\overline{\beta} < \overline{\beta}_c$, we determined the scaling as

对于 $\overline{\beta} < \overline{\beta}_c$，我们得到的标度关系为

$$S^- - 4 = (b_0^-(\varepsilon) + b_1^-(\varepsilon) N)\,\overline{\beta} \tag{17}$$

$$b_0^-(\varepsilon) = 2.09^{(\pm 0.55)}\left(\varepsilon - 0.07^{(\pm 0.01)}\right)^2 - 190.50^{(\pm 15.46)}\left(\varepsilon - 0.07^{(\pm 0.01)}\right)^4$$

(18)

$$b_1^-(\varepsilon) = -0.20^{(\pm 0.06)}\varepsilon^3 - 2.04^{(\pm 0.18)}\varepsilon^2 \tag{19}$$

this remains consistent for all N, ε combinations. The subtraction of 4 from the action makes sense since the expected value for this action on a flat Alexandrov interval is 4, which is due to boundary contributions as examined in [21,22].

该关系对所有 N, ε 组合都成立。作用量减去 4 是合理的: 正如文献 [21,22] 讨论的，平坦 Alexandrov 区间上该作用量的期望值就是 4，这来源于边界贡献。

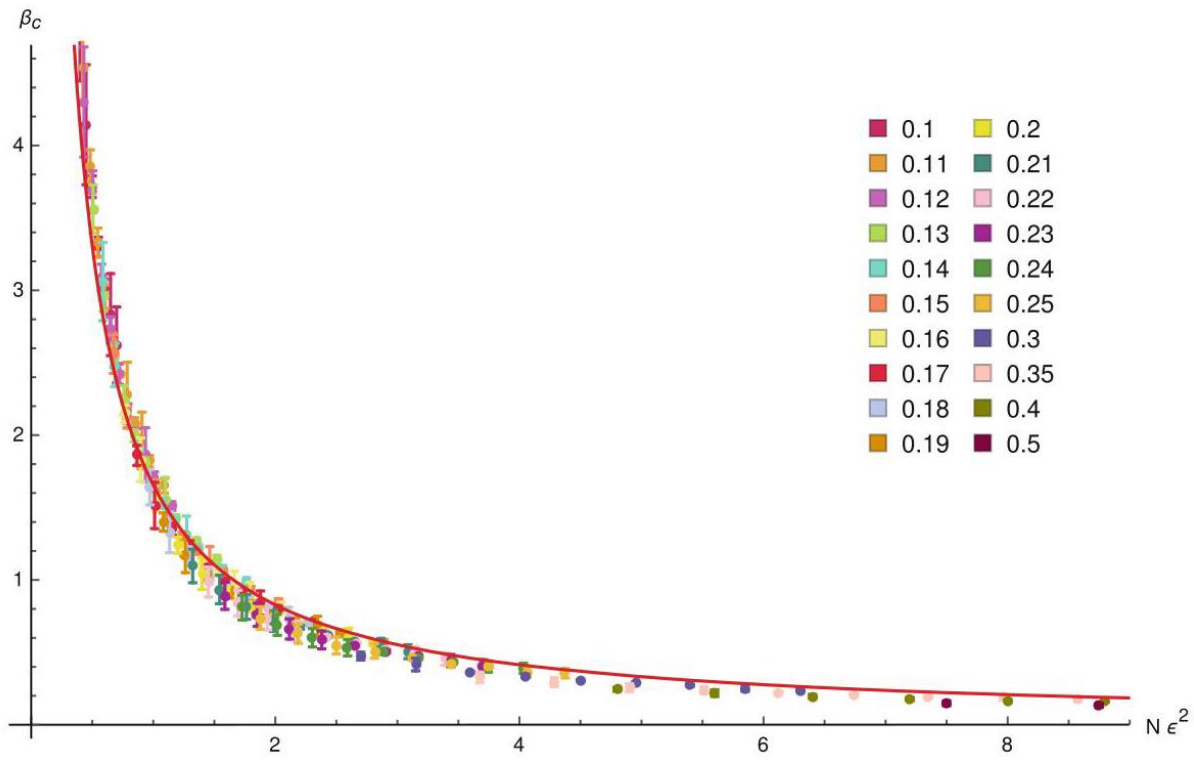

Fig. 5 Plot of the phase transition point β_c for all values of ε plotted against $N\varepsilon^2$ to show that the scaling is an excellent description. The red line shows the best fit scaling

图 5 所有 ε 取值下的相变点 β_c 对 $N\varepsilon^2$ 作图，证明标度关系是非常好的描述。红线展示了最优拟合标度

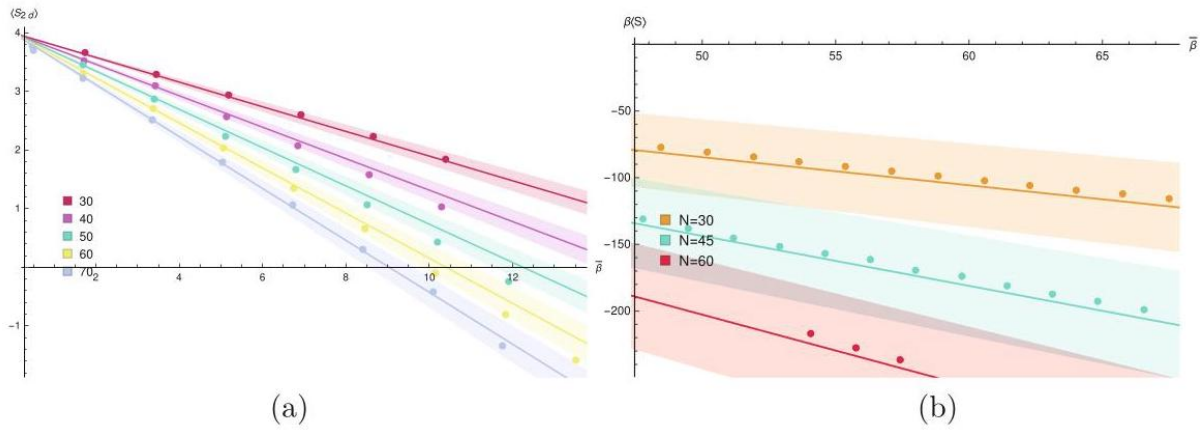

Fig. 6 The left-hand side shows the average action plotted against $\overline{\beta}$ for the region $\beta < \beta_c$, and the right-hand side shows this for $\beta > \beta_c$. The straight lines are best fits and show that the action scales linearly in N for both regions. This scaling remains for all ε with the scaling parameters simple functions of ε . (a) Scaling of $S\beta < \beta_c$. (b) Scaling of $S\beta > \beta_c$

图 6 左侧图绘制了区域 $\beta < \beta_c$ 中平均作用量随 $\overline{\beta}$ 的变化，右侧图为区域 $\beta > \beta_c$ 的对应结果。直线为最佳拟合结果，表明作用量在两个区域中都随 N 线性变化。这种标度关系对所有 ε 都成立，标度参数是关于 ε 的简单函数。(a) $S\beta < \beta_c$ 的标度关系。(b) $S\beta > \beta_c$ 的标度关系

In the region $\overline{\beta} > \overline{\beta}_c$ the scaling is

在区域 $\overline{\beta} > \overline{\beta}_c$ 中，标度关系为

$$\beta S^{+} = a^{+}(N,\varepsilon) + b^{+}(N,\varepsilon)\,\overline{\beta} \tag{20}$$

$$a^{+} = -25.21^{(\pm 8.16)} + 1.53^{(\pm 0.21)} N \tag{21}$$

$$b^{+} = 0.4^{(\pm 0.24)} + 17.63^{(\pm 4.76)}\varepsilon^2 - 2.48^{(\pm 0.09)}\varepsilon^2 N \tag{22}$$

this is consistent with analytic insights one can gain from examining the action on the bilayer orders.

这与我们分析双层有序结构作用量得到的解析结论一致

These fits work well for the action in their respective regions, and we can use finite size scaling to derive scalings for the variance from this, which all confirm the results. We can thus say that we do understand the scaling of the action at the phase transition of the 2 d orders very well.

这些拟合在对应区域都能很好地描述作用量，我们还可以通过有限尺寸标度从中推导出方差的标度关系，所有结果都一致。因此我们可以确定，我们已经充分理解了 2 d 有序结构相变处作用量的标度行为

The Wave Function of a Universe

宇宙波函数

MCMC simulations of the 2d orders can calculate the expectation value of different observables and thus show the phase structure of the theory. In a quantum theory, a typical observation would be a wave function, showing the transition probability from one state to another. In quantum gravity, this is exemplified by the Hartle-Hawking wave function of the universe [23]. The ground state wave function over closed 3 geometries $(\sum, h)$ is the Euclidean functional integral over 4 geometries without an initial boundary

二维序的 MCMC 模拟可以计算不同可观测量的期望值，从而展现该理论的相结构。在量子理论中，典型的可观测量就是波函数，它描述了从一个态到另一个态的跃迁概率。量子引力中的典型例子就是哈特尔-霍金宇宙波函数 [23]。封闭三维几何 $(\sum, h)$ 上的基态波函数，是无初始边界的四维几何上的欧几里得泛函积分

$$\Psi_0\left(\sum, h\right) = A \sum_M \int \mathrm{d}g^E e^{-I_E(g)} \tag{23}$$

where $\partial M = \sum, g|_{\sum} = h$ and $I_E(g)$ is the Euclidean Einstein action. This describes the transition from the no-boundary proposal to a 3 geometry $(\sum, h)$.

其中 $\partial M = \sum, g|_{\sum} = h$ 和 $I_E(g)$ 是欧几里得爱因斯坦作用量。这描述了从无边界提案到三维几何 $(\sum, h)$ 的跃迁。

To establish an equivalent of the HH wave function in a causal set, we need to consider the boundaries; how does a final spatial boundary look in a causal set, and what is the equivalent of no boundary? The simplest proposal for the final boundary is to fix the size of the longest anti-chain without future elements, the final slice of the universe if you will. While, as an anti-chain, this does not directly contain any information about the geometry other than size, the geometric information is encoded in the connectivity to the causal set elements in the past, as shown in [24]. The closest analogue to the no boundary proposal is a single element as an initial condition. This is the choice of initial state that matches up best with the picture of the universe arising from a single point, as described in [25]. Using this we can define the HH wave function in CST as

要在因果集中建立等价的 HH 波函数，我们需要考虑边界：因果集中的最终空间边界是什么样的，无边界的等价形式又是什么？对于最终边界，最简单的提案是固定不存在未来元素的最长反链的大小——你可以将其理解为宇宙的最终切片。反链本身除大小外不直接包含任何几何信息，但正如文献 [24] 所示，几何信息编码在与过去因果集元素的连接关系中。无边界提案最接近的类比是用单个元素作为初始条件。正如文献 [25] 所述，这种初始态选择最符合宇宙从单点诞生的图景。利用这一点我们可以在因果集理论 (CST) 中定义 HH 波函数如下：

$$\Psi_0^{(N)}\left(\mathcal{N}_f,\beta\right)=A\sum_{C\in\Omega_N}e^{\frac{\beta}{\hbar}S(C)}, \tag{24}$$

where here Ω_N is the set of N element causal sets with a single initial element and $\mathcal{N}_f$ final elements. In a first step, we then restrict ourselves to only examine this wave function for the 2 d orders.

其中此处 Ω_N 是带有单个初始元素和 $\mathcal{N}_f$ 个最终元素的 N 元因果集的集合。第一步，我们仅研究该波函数在 2 d 序下的情况。

This is calculated in two steps, first MCMC simulations of the space of all 2d orders with N elements supplemented with analytic methods to obtain an estimate for the partition function $\mathcal{Z}_0\left(\mathcal{N}_f\right)$ of the restricted sets to use for the normalization. Then additional simulations are done to obtain $\langle S_{2d}\rangle_\beta\left(\mathcal{N}_f\right)$, which makes it possible to use numerical integration to calculate the wave function as

该计算分为两步: 首先对包含 N 个元素的所有二维序空间进行 MCMC 模拟，再结合解析方法得到受限集合配分函数 $\mathcal{Z}_0\left(\mathcal{N}_f\right)$ 的估计值，用于归一化。随后通过额外模拟得到 $\langle S_{2d}\rangle_\beta\left(\mathcal{N}_f\right)$，进而可以利用数值积分计算得到波函数:

$$\Psi_0^{(N)}\left(\mathcal{N}_f,\beta\right)=A\mathcal{Z}_\beta\left(\mathcal{N}_f\right)=A\mathcal{Z}_0\left(\mathcal{N}_f\right)\exp^{-\int_0^\beta\langle S_{2d}\rangle_{\beta'1}\left(\mathcal{N}_f\right)\mathrm{d}\beta'}. \tag{25}$$

The normalization uses the partition function for $\beta=0\mathcal{Z}_0\left(\mathcal{N}_f\right)$ and can, up to an irrelevant normalization, be obtained by MCMC simulations. A problem in this approach is that the larger $\mathcal{N}_f$ becomes, the fewer configurations with this state exist.

归一化使用 $\beta=0\mathcal{Z}_0\left(\mathcal{N}_f\right)$ 的配分函数，在相差一个无关归一化常数的范围内，可以通过 MCMC 模拟得到。该方法存在一个问题: $\mathcal{N}_f$ 越大，对应态的构型越少。

In [25], the sets with $N=50$ are explored in depth, since this size has proven a good trade-off between manageable system size and reasonable confidence in our results, in past work. We simulated $1.138\cdot10^{10}$2 d random orders, which led to a sample of 2 d orders with final spatial boundaries of up to $\mathcal{N}_f=19$. We were also capable to calculate the exact number of configurations arising for $\mathcal{N}_f=N-1$, $N-2, N-3$, thus giving us valuable additional information. To obtain a value of $\mathcal{Z}_0$ for all values of $\mathcal{N}_f$, we then used a numerical fit, as shown in Fig. 7. The three analytically obtained points for $\mathcal{N}_f=49,48,47$ are important to anchor this fit, which is used to interpolate intermediate points.

在文献 [25] 中，我们深入探究了包含 $N=50$ 的集合，因为在以往工作中已经证明，该大小在可处理的系统尺寸和结果的合理置信度之间取得了良好的平衡。我们模拟了 $1.138\cdot10^{10}$2 d 个随机序，得到了最终空间边界大小不超过 $\mathcal{N}_f=19$ 的 2 d 个序样本。我们还能够计算得到 $\mathcal{N}_f=N-1$ 、$N-2, N-3$ 对应的精确构型数目，这为我们提供了宝贵的额外信息。为了得到所有 $\mathcal{N}_f$ 取值对应的 $\mathcal{Z}_0$ 值，我们采用了数值拟合，如图 7 所示。$\mathcal{N}_f=49,48,47$ 的三个解析得到的点对固定该拟合十分重要，这些点用于插值得到中间点。

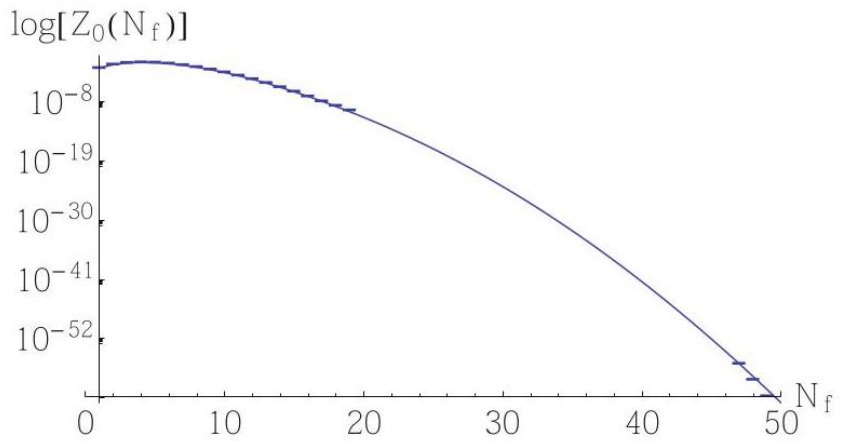

Fig. 7 To determine the normalization factor $\mathcal{Z}_0\left(\mathcal{N}_f\right)$ for arbitrary values of $\mathcal{N}_f$ we generated a sample of configurations and counted the number of occurrences of different $\mathcal{N}_f$ values. To improve the fit we also added values for very large $\mathcal{N}_f$ which were calculated via combinatorial means

图 7 为了确定任意 $\mathcal{N}_f$ 取值下的归一化因子 $\mathcal{Z}_0\left(\mathcal{N}_f\right)$，我们生成了一个组态样本，并统计了不同 $\mathcal{N}_f$ 取值的出现次数。为了提高拟合精度，我们还加入了通过组合方法计算得到的极大 $\mathcal{N}_f$ 对应取值

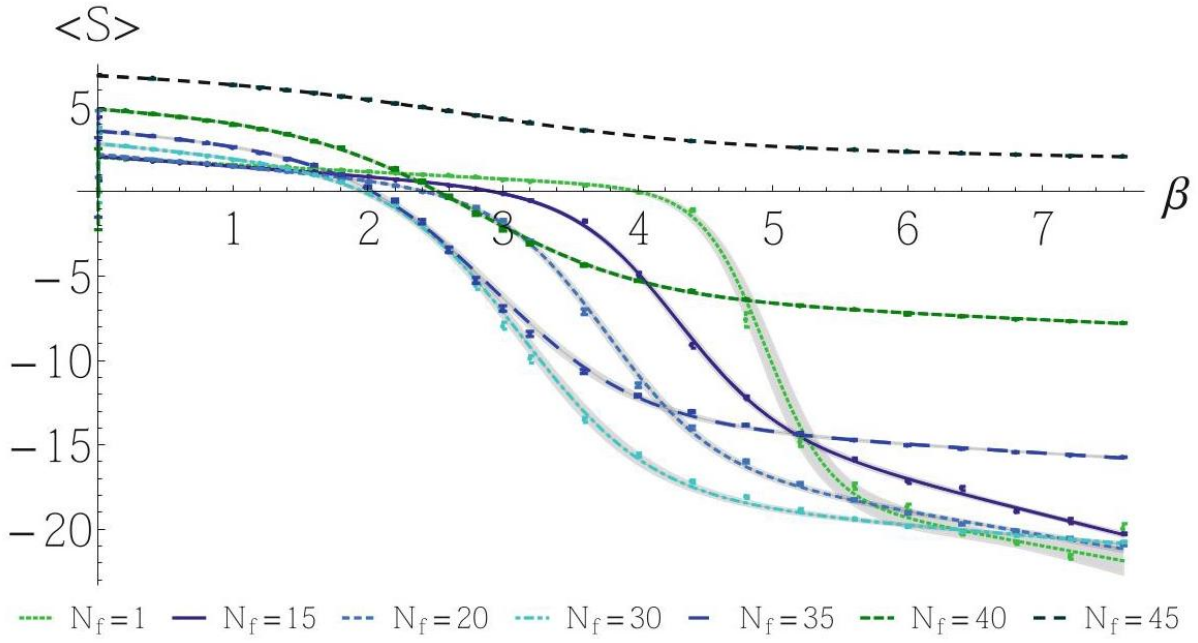

Fig. 8 Average action for a range of $\mathcal{N}_f$ values for $\varepsilon = 0.12$ with their best fit function and shading to show the uncertainty in the fit

图 8 不同 $\mathcal{N}_f$ 取值范围内 $\varepsilon = 0.12$ 的平均作用量，附最佳拟合函数，阴影区域表示拟合的不确定度

After thus having determined $\mathcal{Z}_0\left(\mathcal{N}_f\right)$, we need to determine $\langle S_{2d}\rangle_\beta\left(\mathcal{N}_f\right)$ for a range of $\mathcal{N}_f$ and β. For this we ran separate simulations for each $\mathcal{N}_f, \beta$ combination. We also explored different values of ε, with

the most extensive simulations for $\varepsilon = 0.12$ and some lower resolution simulations for $\varepsilon = 0.5, 1$ to check the consistency of our results. In Fig. 8, we show the data points for a selection of $\mathcal{N}_f$ plotted against β , with the best fit lines and their error regions. The fit is done to obtain a smooth interpolation of the data present, which is necessary to be able to do the integral in (25). In theory splines or other piece wise interpolation methods lead to equivalent results.

确定 $z_0\left(\mathcal{N}_f\right)$ 后，我们需要在一系列 $\mathcal{N}_f$ 和 β 的取值范围内确定 $\langle S_{2d}\rangle_\beta\left(\mathcal{N}_f\right)$。为此我们对每组 $\mathcal{N}_f, \beta$ 组合分别开展了模拟。我们还测试了 ε 的不同取值，对 $\varepsilon = 0.12$ 进行了最高精度的模拟，对 $\varepsilon = 0.5, 1$ 进行了低精度模拟，以检验我们结果的一致性。在图 8 中，我们展示了部分 $\mathcal{N}_f$ 的数据点，以 β 为横轴作图，附最佳拟合线及其误差区域。拟合是为了对现有数据进行平滑插值，这是完成 (25) 式积分的必要步骤。从理论上讲，样条插值或其他分段插值方法可以得到等价结果。

Using this function, we numerically integrated, utilizing Mathematica, to obtain numerical values for $\Psi_0\left(\mathcal{N}_f, \beta\right)$. These are shown in Fig. 9, where the wave function of the universe is peaked around different final configurations for different β .

借助该函数，我们使用 Mathematica 进行了数值积分，得到了 $\Psi_0\left(\mathcal{N}_f, \beta\right)$ 的数值结果。结果如图 9 所示，不同 β 对应的宇宙波函数峰值出现在不同的终组态处。

The first peak is around $\mathcal{N}_f \sim 4$ and is dominant for low β and consists of the random, manifoldlike 2d orders, which we already observed above. The second peak is around $\mathcal{N}_f \sim 23$ and dominates once β becomes high enough. We show examples of typical causal sets in either of these peaks in Fig. 10.

第一个峰值位于 $\mathcal{N}_f \sim 4$ 附近，在低 β 时占主导，由我们上文已经观测到的随机类流形二维序构成。第二个峰值位于 $\mathcal{N}_f \sim 23$ 附近，当 β 足够大时占主导。我们在图 10 中展示了分别位于两个峰值的典型因果集示例。

The causal sets in the 2nd peak are similar to those in the crystalline phase but restricted by our initial condition of $\mathcal{N}_i = 1$. These configurations show several properties that are physically interesting. They are rapidly expanding, as determined by the ratio of the largest anti-chain to the longest chain in the set. It would be interesting to see how this would continue for larger N . Another suggestive property of these causal sets is the distribution of pasts, as shown in Fig. 11. The histogram shows the average distribution of past volumes for the final elements for $\mathcal{N}_f = 23, \beta = 7.6$. On average each of the final elements is connected to almost all other elements in the causal set. This high connectivity leads to a very homogeneous initial condition on this slice of the universe, similar to what is also achieved through inflation. This is an interesting hint that discreteness in the early universe could give rise to the homogeneity of the universe.

第二个峰值中的因果集与晶相的因果集类似，但受到我们 $\mathcal{N}_i = 1$ 初始条件的限制。这些组态具有多个值得物理关注的性质。根据因果集中最大反链与最长链的比值判断，它们处于快速膨胀状态。探究更大的 N 下这一性质会如何延续会很有意义。这些因果集的另一个值得关注的性质是过去分布，如图 11 所示。直方图展示了 $\mathcal{N}_f = 23, \beta = 7.6$ 下最终元素的过去体积平均分布。平均来看，每个最终元素几乎连接了因果集中所有其他元素。这种高连通性使得宇宙该切片上的初始条件非常均匀，与暴胀产生的效果类似。这是一个有意思的提示，说明早期宇宙的离散性可以促成宇宙的均匀性。

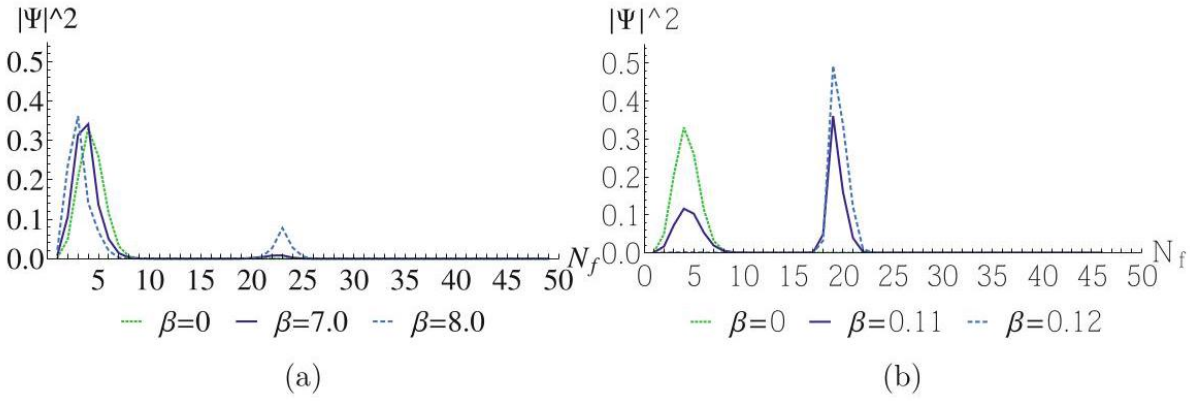

Fig. 9 Wave function for different values of β , showing how the wave function is concentrated around two peaks, one of which is dominant for small β while the other becomes dominant at larger β . (a) $\varepsilon = 0.12$. (b) $\varepsilon = 0.5$

图 9 不同 β 取值对应的波函数，展示了波函数集中在两个峰值附近，其中一个峰值在小 β 时占主导，另一个峰值在大 β 时占主导。(a) $\varepsilon = 0.12$ 。(b) $\varepsilon = 0.5$

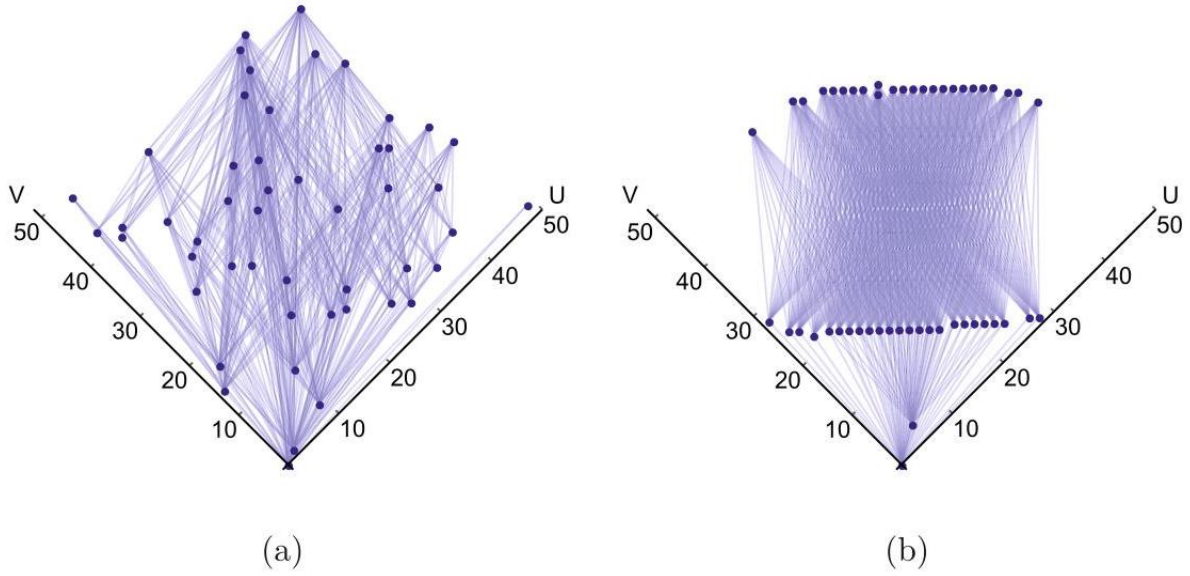

Fig. 10 Typical causal sets taken from the two peaks in the wave function for $\varepsilon = 0.12$. For low β the typical configuration is random, while the typical configuration for large β shows rapid expansion, and a crystalline behavior. (a) $\mathcal{N}_f = 4, \beta = 0.2$. (b) $\mathcal{N}_f = 23, \beta = 7.6$

图 10 取自 $\varepsilon = 0.12$ 波函数两个峰值的典型因果集。低 β 下的典型构型是随机的，而大 β 下的典型构型呈现快速膨胀和晶体性行为。(a) $\mathcal{N}_f = 4, \beta = 0.2$ 。(b) $\mathcal{N}_f = 23, \beta = 7.6$

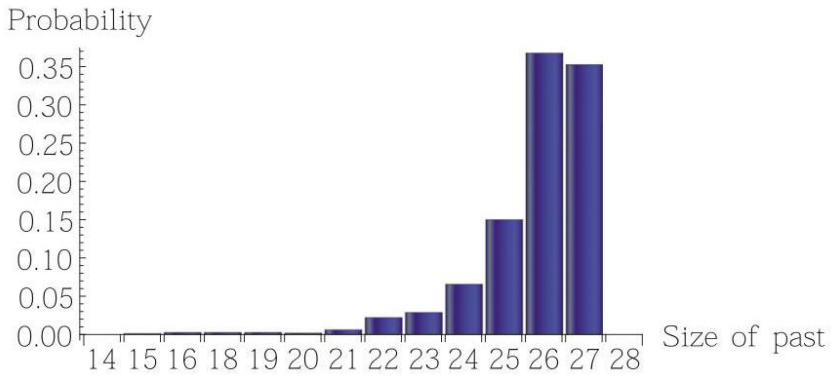

Fig. 11 Probability histogram for the size of the past of a final element in the large β dominant state. This shows that most final elements contain all bulk elements in their past

图 11 大 β 主导态中末元素过去集合大小的概率直方图。图中表明，大多数末元素的过去集合包含所有体元

Adding Matter - The Ising Model

添加物质——伊辛模型

The studies above demonstrate that the 2 d orders are a great testing ground to explore causal sets using computer simulations. This can be taken even further. One big question in causal set theory is, how to incorporate matter in the theory, and the 2d orders let us explore this. In particular, we can define an Ising type model, by assigning a "spin," a variable with values $[+1, -1]$ to each causal set element. The interaction term for these can then be defined using the link matrix L_{ij}

上述研究表明，2 d 序是利用计算机模拟探索因果集的绝佳试验场。我们还可以更进一步。因果集理论中的一个核心问题是如何在理论中纳入物质，而二维序让我们能够对这一问题开展探索。具体而言，我们可以定义一个伊辛类模型: 为每个因果集元素分配一个“自旋”，即取值为 $[+1, -1]$ 的变量。之后可以利用链接矩阵 L_{ij} 定义这些自旋的相互作用项

$$S_{\text{Ising}} = j \sum_{k,l \in \mathcal{C}} s_k L_{kl} s_l = j \sum_{k \prec l} s_k s_l, \tag{26}$$

to obtain a spin interaction along links [26,27].

从而得到沿链接的自旋相互作用 [26,27]。

This makes it possible to study how the systems of matter and geometry interact, whether they give rise to new phases, and how the transitions between these phases behave. It is particularly salient to examine if the transitions might become of higher order, since smooth phase transitions allow for a continuum limit. While a continuum limit is not necessary for causal set theory, it does give more analytical tools to examine a theory.

这使得我们可以研究物质与几何系统如何相互作用，二者是否会产生新相，以及这些相之间的相变有何性质。考察相变是否为高阶相变尤其重要，因为平滑的相变可以存在连续极限。连续极限对因果集理论而言并非必要条件，但它确实能为理论研究提供更多分析工具。

A priori the Ising model has three possible states, spins can be correlated along links, anti-correlated along links, or uncorrelated, while the 2d orders have two phases we know so far, the random 2d orders and the crystalline orders. If these phases arise in all combinations, without giving rise to any new behaviors, we would expect to find six phases in the coupled system

伊辛模型先验地存在三种可能状态: 自旋沿链接关联、沿链接反关联或无关联；而二维序目前已知存在两个相，即随机二维序和晶序。如果这些相可以任意组合、不产生新行为，我们预期耦合系统将存在六个相

To study these phases, in addition to the observables already used to study the 2d orders, we also examined the Ising action (26), and the absolute magnetization of the system

为研究这些相，除了已经用于研究二维序的可观测量外，我们还检验了伊辛作用量 (26) 和系统的绝对磁化强度

$$|M| = \left| \frac{1}{N} \sum_i s_i \right| \tag{27}$$

The phase structure as found in [26] is shown in Fig. 12, where we see that only five different phases can be identified. For the studies, we explored $\varepsilon = 0.21$, since the prior studies of the 2 d orders without matter make us confident that there will be no qualitative change in the orders with ε , as long as it is not chosen very small.

文献 [26] 中得到的相结构如图 12 所示,我们只能从中识别出五个不同的相。在研究中我们对 $\varepsilon = 0.21$ 进行了探索，因为此前对不含物质的 2 d 序的研究让我们确信，只要 ε 不选得太小，含 ε 的序不会发生定性改变。

In the region around $\beta = j = 0$, we find random 2 d orders with uncorrelated Ising spins; this is the region where both systems are dominated by the entropy of configurations. As β increases while j stays close to 0, we find a transition to the crystalline 2 d orders, with uncorrelated Ising spins on them. If j increases, we find crystalline causal sets with anti-correlated spins, while negative j induces crystalline 2d orders with correlated spins.

在 $\beta = j = 0$ 附近区域，我们得到了带有无关联伊辛自旋的随机 2 d 序；该区域中两个系统都由构型熵主导。当 β 增大而 j 保持接近 0 时，我们发现系统跃迁到带有无关联伊辛自旋的晶体 2 d 序。如果 j 增大，我们得到带有反关联自旋的晶体因果集；而负 j 会诱导出带有关联自旋的晶体二维序。

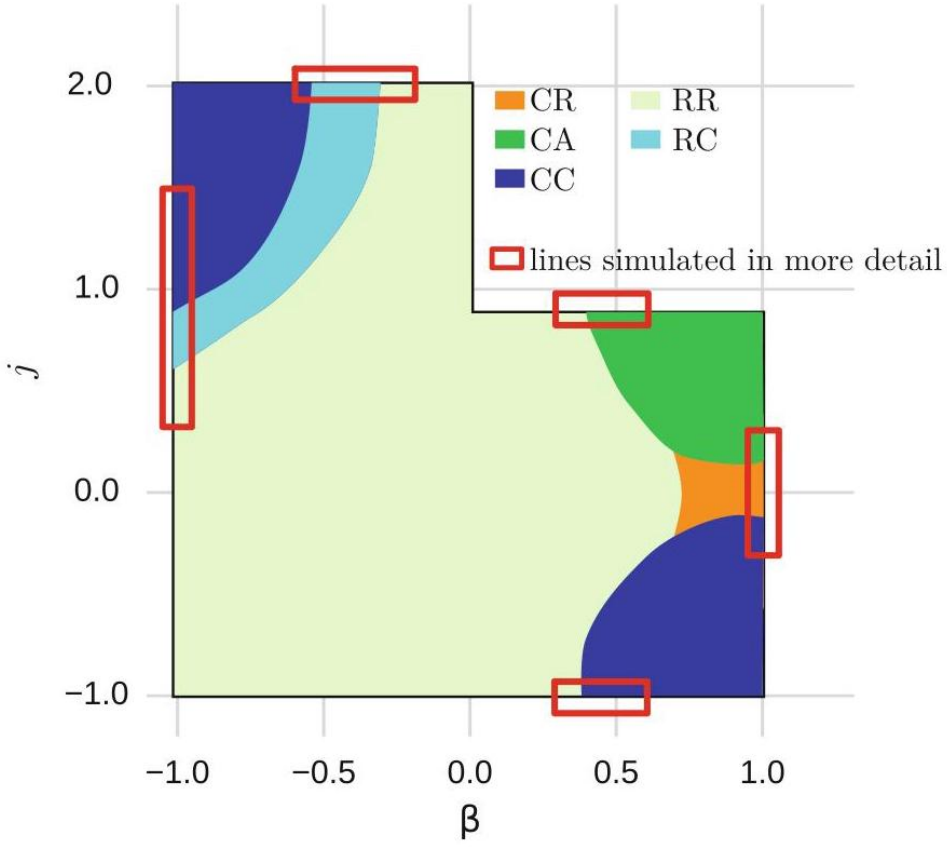

Fig. 12 Phase diagram of the system of the Ising model coupled to the 2 d orders. The light green region RR is random 2 d orders with uncorrelated Ising spins; the vibrant green region CA is crystalline 2d orders with anti-correlated Ising spins; the orange region CR is crystalline causal sets with uncorrelated Ising spins; the dark blue region CC is crystalline causal sets with correlated Ising spins; and the cyan region RC is random 2d orders with correlated Ising spins. The red boxes mark lines that were studied in more detail. (This figure is taken from [26])

图 12 耦合 2 d 序的伊辛模型系统的相图。浅绿色区域 RR 是带有无关联伊辛自旋的随机 2 d 序；深绿色区域 CA 是带有反关联伊辛自旋的晶体二维序；橙色区域 CR 是带有无关联伊辛自旋的晶体因果集；深蓝色区域 CC 是带有关联伊辛自旋的晶体因果集；青色区域 RC 是带有关联伊辛自旋的随机二维序。红色框标记了已开展更详细研究的线。(本图引自文献 [26])

Since β is a free parameter in this model, we also extended the study to negative β . We find that for $j = 0$ and $\beta \in [0, -1]$ the 2 d orders still behave as random orders, without a clear phase transition. The negative j and negative β region does not show any signs of a new phase arising. However, this region should give rise to anti-correlated spins, which are harder to examine using the observables defined above, so it is possible that interesting behavior has not been found.

由于 β 是该模型的自由参数，我们还将研究扩展到了负 β 的情况。我们发现，对于 $j = 0$ 和 $\beta \in [0, -1]$ ，2 d 序仍然表现为随机序，不存在清晰的相变。负 j 和负 β 区域没有出现新相的迹象。但该区域本应产生反关联自旋，反关联自旋很难用上述可观测量研究，因此可能还有有趣的行为尚未被发现。

For positive j and negative β , we find the most intriguing behavior. Without the Ising model, the path

sum in this region would still be dominated by random orders, while the Ising action favors maximizing the number of links, and thus creating crystalline orders. These competing effects give rise to a double phase transition from random 2d orders with disordered spins, to random 2d orders with ordered spins, to crystalline 2d orders with ordered spins, which is a matter induced phase transition of geometry.

对于正 j 和负 β，我们发现了最值得关注的行为。如果没有伊辛模型，该区域的路径和仍然由随机序主导，而伊辛作用量倾向于最大化链接数，从而促成晶体序。这些竞争效应引发了双重相变: 从带无序自旋的随机二维序，到带有序自旋的随机二维序，再到带有序自旋的晶体二维序，这是物质诱导的几何相变。

This process and the order of this induced phase transition was studied closer in [27]. To do so we simulated the system at different sizes ranging from $N = 20$ to $N = 120$, for a line at $j = -1$ and one line along $j = 1$.

文献 [27] 对这一过程以及该诱导相变的顺序开展了更深入的研究。为此我们在尺寸范围从 $N = 20$ 到 $N = 120$ 的系统中进行了模拟，对应 $j = -1$ 处的一条线与沿 $j = 1$ 的一条线。

Along the line $j = -1, \beta \in [0, 0.8]$, we find one phase transition, from a phase in which both the Ising spins and the geometry are random, into a phase in which the Ising spins are aligned, and the causal set is crystalline.

沿 $j = -1, \beta \in [0, 0.8]$ 这条线，我们发现了一处相变: 系统从伊辛自旋与几何均为随机的相，转变为伊辛自旋对齐、因果集为晶态的相。

Studying this phase transition in detail, we found that the phase transition happens at smaller β values than for the pure 2d order system, and scales like

通过详细研究该相变，我们发现该相变发生在比纯二维序系统更小的 β 值处，其标度行为满足

$$\beta_c(N) = (3.35 \pm 0.15) \cdot N^{-0.72 \pm 0.01}. \tag{28}$$

This odd scaling in N is likely an effect of the Ising model slowing the scaling as compared to that expected for the pure 2d orders.

N 的这种反常标度很可能源于伊辛模型相较于纯二维序的预期放缓了标度过程。

Looking at the Binder cumulant of the observables in Fig. 13, we see that the transition appears of first order in the observables associated with geometry, but of higher order in those associated with the Ising spins.

观察图 13 中可观测量的宾德累积量，我们可以看到，与几何关联的可观测量显示该相变是一级相变，而与伊辛自旋关联的可观测量则显示它是高阶相变。

This leads us to the conclusion that this is a mixed order phase transition. While the transitions remain different in the two parts of the system, one cannot deny that the systems are strongly influencing each other, since the location of the transition and the scaling of this location with the system size are changed considerably compared to the uncoupled systems.

这让我们得出结论: 该相变是混合级相变。尽管系统两个部分的相变仍然不同，但无法否认两个系统存在强烈的相互影响: 与无耦合的系统相比，相变的位置以及该位置随系统尺寸的标度都发生了显著变化。

Studying the scaling of the system with size shows that the actions scale linearly in N in the low β region where causal sets and spins are random and quadratic in N in the crystalline and correlated region at high β .

研究系统随尺寸的标度行为可知: 在低 β 区域，作用量随 N 线性标度，该区域中因果集和自旋均为随机；在高 β 的晶态关联区域，作用量随 N 二次标度。

The other line explored is $j = 1, \beta \in [-1.4, 0]$, which crosses two phase transitions, including one induced by the Ising model. At high β , we observed a magnetic transition from a phase of uncorrelated spins and random 2 d orders to a phase of random 2 d orders and correlated spins, which is followed by a geometric transition as β is further decreased. This transition goes from random 2 d orders with correlated spins to crystalline 2 d orders with correlated spins.

我们探究的另一条线是 $j = 1, \beta \in [-1.4, 0]$ ，它穿过两处相变，其中一处由伊辛模型诱导。在高 β 处，我们观测到从自旋无关联、2 d 序随机的相到 2 d 序随机、自旋关联的相的磁性相变；进一步降低 β 后，会发生几何相变，从 2 d 序随机、自旋关联的相转变为 2 d 序晶态、自旋关联的相。

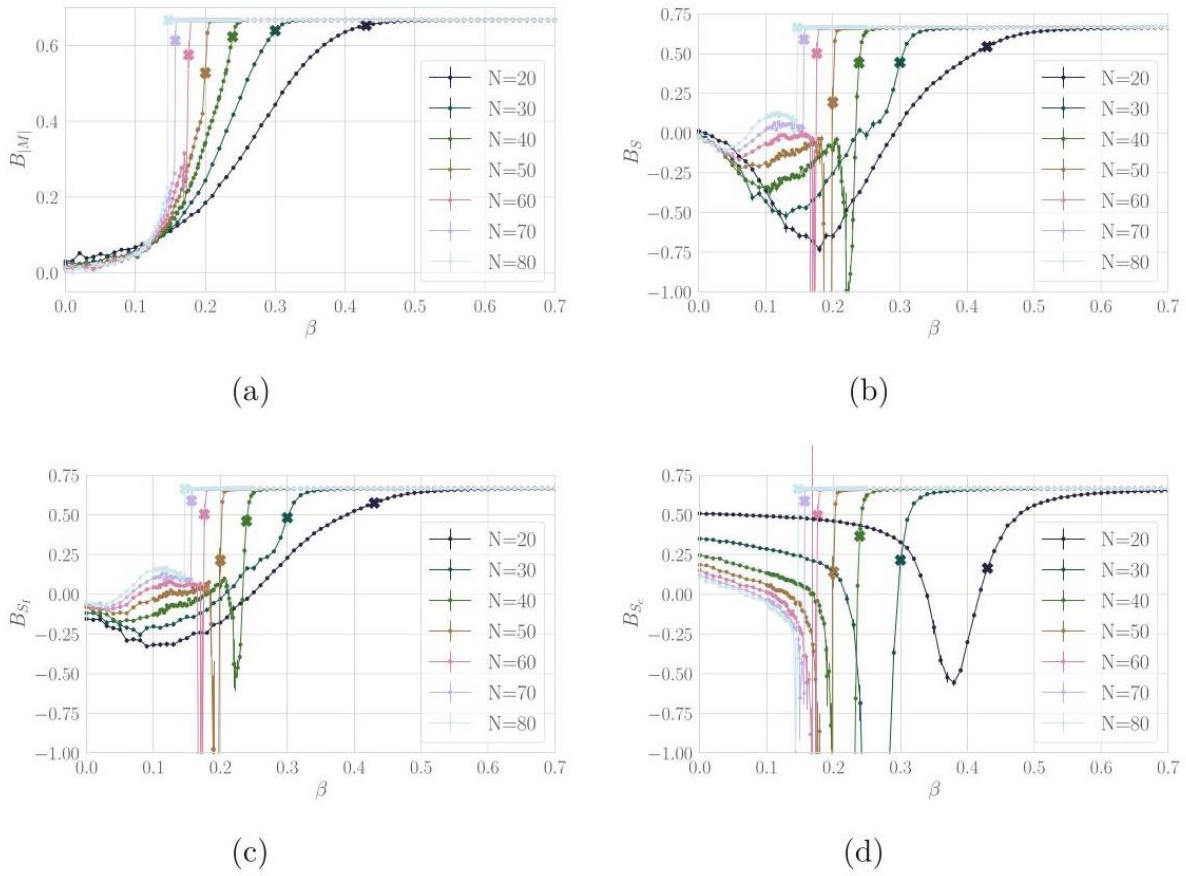

Fig. 13 The fourth-order cumulant for the actions and the magnetization at $j = -1$. The thicker crosses indicate the location of the phase transition, as determined from the peak of Var (S) . (a) B_M . (b) B_S . (c) B_{S_I}

. (d) B_{S_c}

图 13 $j = -1$ 处作用量和磁化强度的四阶累积量。粗十字标记出由 Var (S) 峰确定的相变位置。(a) B_M。(b) B_S。(c) B_{S_I}。(d) B_{S_c}

The scaling of the transitions with N can be fit as

相变随 N 的标度可拟合为

$$\beta_{c,mag} = (-1.22 \pm 0.20) \cdot N^{-0.41 \pm 0.04} \tag{29}$$

$$\beta_{c,geo} = (-8.58 \pm 0.34) \cdot N^{-0.77 \pm 0.01} \tag{30}$$

Extrapolating these fits to very high N , the lines would meet somewhere between $N \sim 500 - 1000$, depending on the error bars of the fits. However, physically this seems to be unlikely, since the spins need to align before they can force the 2d order into a crystalline structure, we expect that the extrapolation is flawed and that the distinct phases will persist at large N .

将这些拟合外推到极高 N，两条线会交汇在 $N \sim 500 - 1000$ 之间的某处，具体位置取决于拟合的误差棒。但这在物理上似乎并不合理: 自旋需要先对齐才能迫使二维序形成晶体结构，因此我们认为该外推存在缺陷，在大 N 下不同的相仍会持续存在。

Exploring the transitions closer, we see that the observables are consistent with a higher order phase transition, apart from the histogram of the action whose distribution grows wider as N increases, instead of peaking sharply. The transition of geometry, however, still is appears consistent with a first-order transition. Both phase transitions can be seen in the Binder coefficients shown in Fig. 14.

进一步探究相变后我们发现，除了作用量的分布会随 N 增大变宽而非尖锐成峰外，其余可观测量均与高阶相变一致。而几何相变的结果仍然符合一级相变的特征。两种相变都可以在图 14 所示的宾德系数中观察到。

So while matter can induce a phase transition in geometry, it does not fundamentally change the type of transition that geometry undergoes, in this context.

因此在此框架下，尽管物质可以诱导几何发生相变，但它并未从根本上改变几何发生的相变类型。

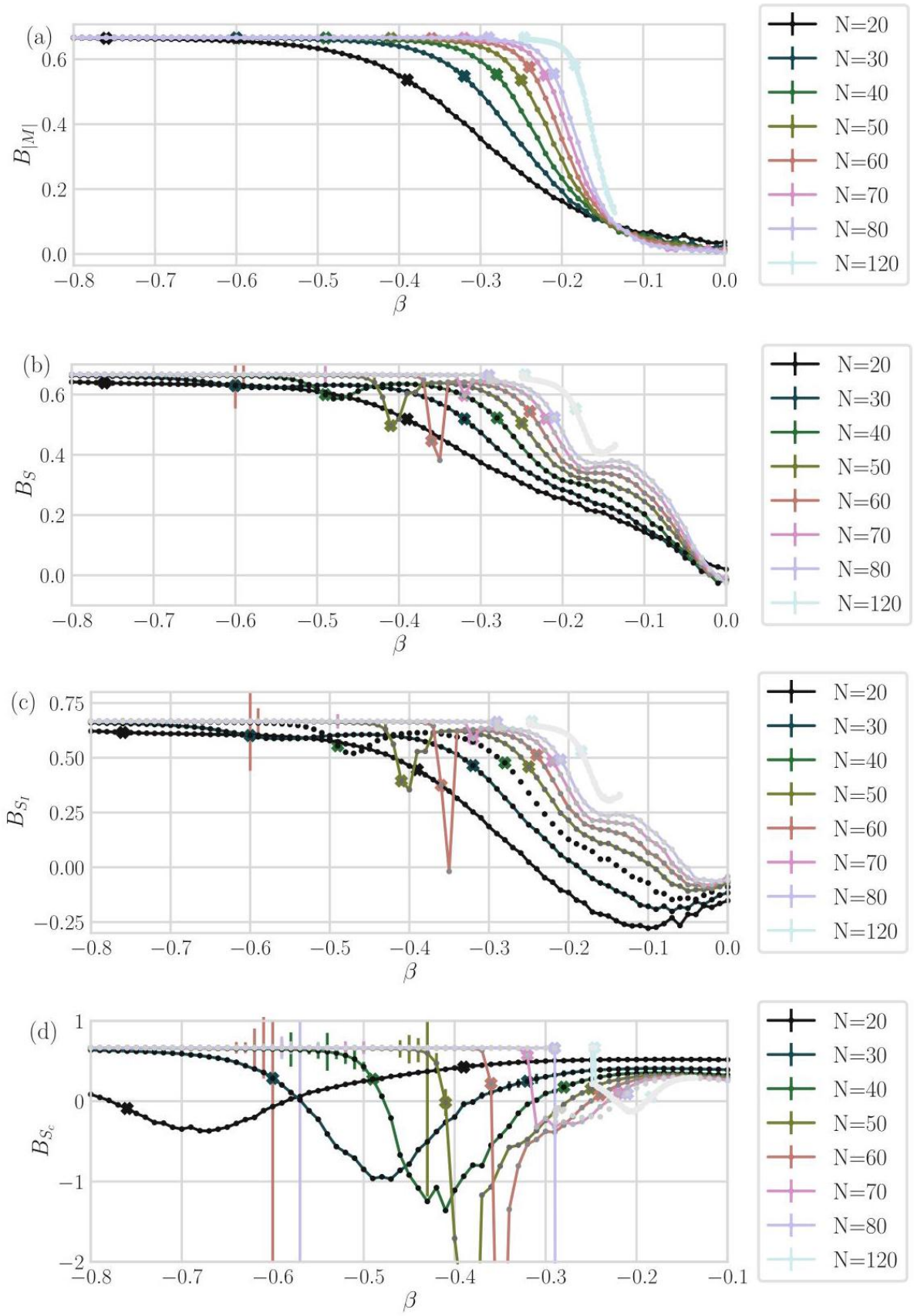

Fig. 14 Fourth-order cumulant plotted against β for both the action and the magnetization for $j = 1$. The thicker crosses indicate the two phase transition points. The rightmost cross of each color is the magnetic

transition, while the second cross indicates the geometric transition, both measured using the peaks in the Variance Var (S) . (a) B_M . (b) B_S . (c) B_{S_I} . (d) B_{S_c}

图 14 针对 $j = 1$ ，将四阶累积量按作用量和磁化强度分别对 β 作图。更粗的十字标记两个相变点。每种颜色最右侧的十字是磁相变，第二个十字是几何相变，二者均通过方差 Var (S) 的峰值测定。(a) B_M 。(b) B_S 。(c) B_{S_I} 。(d) B_{S_c}

Examining the scaling of the action it is found to be identical to that of the random uncorrelated and the crystalline correlated phases, respectively, along the negative j line. For the region of random causal sets with correlated spins, we did not find any clear scaling.

研究作用量的标度行为发现，沿负 j 线，其标度分别与无关联随机相和结晶关联相的标度一致。对于自旋关联的随机因果集区域，我们未发现任何清晰的标度行为。

The work thus shows that coupling the Ising model to the 2d orders does not fundamentally disrupt the scaling behavior. While we do find some new phase transitions, they do not seem to be of higher order in geometry and do thus not resolve the problem of predictability mentioned above. It is, however, promising that they do show strong coupling between matter and geometry, thus allowing us to study a coupled system. More work is certainly needed to understand more realistic matter on more realistic causal sets.

因此该研究表明，将伊辛模型耦合到二维序中不会从根本上破坏标度行为。尽管我们确实发现了一些新的相变，但它们在几何上似乎并非高阶相变，因此无法解决前文提到的可预测性问题。但值得欣喜的是，它们确实展现出物质与几何之间的强耦合，这让我们得以研究耦合系统。要理解更真实因果集上更真实的物质，无疑还需要开展更多研究。

Outlook

展望

This chapter has introduced MCMC simulations on the 2 d orders as a model system of causal sets. Even this simple case still leaves many interesting open questions for future investigation. First we should further our understanding of matter on this simple system. This could take the form of including a scalar field, either using the d'Alembertian operator defined above (10) or using the Greens function as described in the chapters on quantum field theory on causal sets by Nomaan X and Ian Jubb. It would also be physically interesting to see how the wave function of the universe is influenced by the inclusion of matter.

本章介绍了作为因果集模型系统的 2 d 序上的 MCMC 模拟。即便是这个简单情形，仍留下了许多有趣的开放性问题供未来研究。首先，我们需要进一步理解这个简单系统中的物质问题: 具体可以引入标量场，既可以采用前文定义的达朗贝尔算符 (10)，也可以使用 Nomaan X 和 Ian Jubb 所著因果集量子场论章节中介绍的格林函数。研究引入物质后对宇宙波函数的影响在物理上也十分有意义。

The model of the 2d orders can also be extended, allowing for more general configurations and thus moving closer toward the physically interesting case of four dimensional space-time. This is done in the lattice gas model defined in [28]. 2d orders as a lattice, with N^2 lattice sites of which only N are occupied, but each occupied site precludes other elements sharing the same light-cone coordinates, which since there are

only N possible values for each coordinate means that with N elements there can be no additional elements added still satisfying the conditions. The generalized lattice gas extends the configuration space by allowing for elements to share coordinates and by decoupling the number of lattice sites from the number of elements.

二维序模型还可以进行拓展，以容纳更一般的构型，从而更接近四维时空这个物理上备受关注的情形。拓展工作已在文献 [28] 定义的晶格气模型中完成。二维序作为晶格，共有 N^2 个格点，其中仅有 N 个被占据，每个被占据格点不允许其他元素共享同一光锥坐标；由于每个坐标仅有 N 种可能取值，因此当存在 N 个元素后，无法再添加满足条件的新元素。推广的晶格气通过允许元素共享坐标、解耦格点数量与元素数量拓展了构型空间。

This also allows for an extension to causal sets in higher dimensions. In general extending the 2d orders to 3 or higher dimensions is not a good model of space-time, since it would lead to ”hypercube light cones.” This implies that causal sets that approximate 3 d space-time are not included in the 3 d orders, since their causality structure is not represented. However, the more general lattice models allow for empty lattice sites and thus do include manifoldlike configurations. In particular the limit of taking the number of lattice sites to infinity for a fixed size of the causal set recovers the case of a sprinkling into flat Minkowski space. The generalized lattice model also opens the possibility of exploring changes in the topology of our configurations.

这也能将模型拓展至高维因果集。一般来说，将二维序拓展至三维或更高维度并不是描述时空的好模型，因为这会产生“超立方光锥”，这意味着近似 3 d 时空的因果集无法被纳入 3 d 序，其因果结构无法被表达。但更一般的晶格模型允许存在空格点，因此可以容纳流形类构型，特别是对于固定大小的因果集取格点数量趋于无穷的极限，就可以得到向平直闵氏空间撒播因果集的结果。推广的晶格模型也为探索构型的拓扑变化提供了可能。

References

参考文献

1. D.P. Rideout, R.D. Sorkin. A Classical sequential growth dynamics for causal sets. Phys. Rev. D 61, 024002 (2000). https://doi.org/10.1103/PhysRevD.61.024002, arXiv: gr-qc/9904062

2. J. Ambjorn, A. Goerlich, J. Jurkiewicz, R. Loll. Nonperturbative quantum gravity. Phys. Rep. 519(4-5), 127-210 (2012). arXiv: 1203.3591, ISSN: 03701573, https://doi.org/10.1016/j.physrep.2012.03.007

3. D.J. Kleitman, B.L. Rothschild, Asymptotic enumeration of partial orders on a finite set. Trans. Am. Math. Soc. 205, 205-220 (1975). ISSN: 0002-9947

4. J. Henson, D.P. Rideout, R.D. Sorkin, S. Surya, Onset of the asymptotic regime for finite orders. Exp. Math. 26(3), 253-266 (2015). arXiv: 1504.05902, https://doi.org/10.1080/10586458.2016.1158134

5. A. Mathur, A.A. Singh, S. Surya, Entropy and the link action in the causal set path-sum. Class. Quant. Grav. 38(4), 045017 (2021). https://doi.org/10.1088/1361-6382/abd300, arXiv: 2009.07623[gr-qc]

6. G. Brightwell, J. Henson, S. Surya, A 2D model of causal set quantum gravity: the emergence of the continuum. Class. Quant. Grav. 25(10), 105025 (2008). ISSN: 0264-9381, https://doi.org/10.1088/0264-9381/25/10/105025

7. P. Winkler, Random orders. Order 1(4), 317-331 (1985). ISSN: 1572-9273, https://doi.org/10.1007/BF00582738

8. R.D. Sorkin, Does locality fail at intermediate length-scales, in Approaches to Quantum Gravity, ed. by D. Oriti (Cambridge University Press, 2007), pp. 26-43. arXiv: gr-qc/0703099, http://arxiv.org/abs/gr-qc/0703099.

9. D.M.T. Benincasa, F. Dowker, Scalar curvature of a causal set. Phys. Rev. Lett. 104(18), 181301 (2010). https://doi.org/10.1103/PhysRevLett.104.181301

10. F. Dowker, L. Glaser, Causal set d'Alembertians for various dimensions. Class. Quant. Grav. 30(19), 195016 (2013). ISSN: 0264-9381, https://doi.org/10.1088/0264-9381/30/19/195016

11. L. Glaser, A closed form expression for the causal set d'Alembertian. Class. Quant. Grav. 31, 095007 (2014). https://doi.org/10.1088/0264-9381/31/9/095007

12. L. Glaser, S. Surya, Towards a definition of locality in a manifoldlike causal set. Phys. Rev. D88, 124026 (2013). https://doi.org/10.1103/PhysRevD.88.124026.This article is reproduced in Appendix refapp: Local

13. R.D. Sorkin, Is the spacetime metric Euclidean rather than Lorentzian?, Is the Spacetime Metric Euclidean Rather than Lorentzian?, ed. by A. Dasgupta (Nova Science Publishers, NY, 2012), pp. 115-135. ISBN: 978-1-61942-392-3, http://arxiv.org/abs/0911.1479

14. S. Surya, Evidence for the continuum in 2D causal set quantum gravity. Class. Quant. Grav. 29(13), 132001 (2012). ISSN: 0264-9381, https://doi.org/10.1088/0264-9381/29/13/132001

15. L. Glaser, Isingcauset. https://github.com/LisaGlaser/IsingCauset

16. M.E.J. Newman, G.T. Barkema, Monte Carlo Methods in Statistical Physics (Clarendon Press, Oxford, 1999). ISBN: 978-0-19-851797-9

17. L. Machet, J. Wang, On the continuum limit of Benincasa-Dowker-Glaser causal set action. Class. Quant. Grav. 38(1), 015010 (2020). https://doi.org/10.1088/1361-6382/abc274, https:// doi.org/10.1088%2F1361-6382%2Fabc274

18. L. Glaser, D. O'Connor, S. Surya, Finite size scaling in 2d causal set quantum gravity. Class. Quant. Grav. 35(4), 045006 (2018). ISSN: 0264-9381. https://doi.org/10.1088/1361- 6382/aa9540

19. K. Binder, Critical properties from monte carlo coarse graining and renormalization. Phys. Rev. Lett. 47(9), 693-696 (1981). https://doi.org/10.1103/PhysRevLett.47.693

20. A. Eichhorn, Towards coarse graining of discrete Lorentzian quantum gravity. Class. Quant. Grav. 35(4), 044001 (2018). arXiv: 1709.10419, ISSN: 0264-9381, 1361-6382. https://doi.org/ 10.1088/1361-6382/aaa0a3

21. D.M.T. Benincasa, F. Dowker, B. Schmitzer, The random discrete action for two-dimensional space-time. Class. Quant. Grav. 28(10), 105018 (2011). https://doi.org/10.1088/0264-9381/28/ 10/105018, https://doi.org/10.1088%2F9381%2F28%2F10%2F105018

22. M. Buck, F. Dowker, I. Jubb, S. Surya, Boundary terms for causal sets. Class. Quant. Grav. 32(20), 205004 (2015). arXiv: 1502.05388, ISSN: 0264-9381, 1361-6382. https://doi.org/10.1088/0264-9381/32/20/205004

23. J.B. Hartle, S.W. Hawking, Wave function of the Universe. Phys. Rev. D 28(12), 2960-2975 (1983). https://doi.org/10.1103/PhysRevD.28.2960

24. S. Major, D. Rideout, S. Surya, Stable homology as an indicator of manifoldlikeness in causal set theory. Class. Quant. Grav. 26(17), 175008 (2009). ISSN: 0264-9381. https://doi.org/10.1088/0264-9381/26/17/175008

25. L. Glaser, S. Surya, The Hartle-Hawking wave function in 2D causal set quantum gravity. Class. Quant. Grav. 33(6), 065003 (2016). ISSN: 0264-9381, https://doi.org/10.1088/0264- 9381/33/6/065003

26. L. Glaser, The Ising model coupled to 2d orders. Class. Quant. Grav. 35(8), 084001 (2018). ISSN: 0264-9381, https://doi.org/10.1088/1361-6382/aab139

27. L. Glaser, Phase transitions in 2d orders coupled to the Ising model. Class. Quant. Grav. 38(14), 145017 (2021). arXiv: 2011.13875, ISSN: 0264-9381, 1361-6382. https://doi.org/10.1088/1361-6382/abf1c5

28. W.J. Cunningham, S. Surya, Dimensionally restricted causal set quantum gravity: examples in two and three dimensions. Class. Quant. Grav. 37(5), 054002 (2020). ISSN: 0264-9381. https:// doi.org/10.1088/1361-6382/ab60b7